Probabilistic Tsunami Hazard Analysis for Tuzla Test Site Using Monte Carlo Simulations

Hafize Basak Bayraktar[1,2,3], Ceren Ozer Sozdinler[4]

[1]Department of Geophysics, Kandilli Observatory and Earthquake Research Institute, Bogazici University, Istanbul, 34684, Turkey
[2]Department of Physics "Ettore Pancini", University of Naples Federico II, Naples, 80126, Italy
[3]Istituto Nazionale di Geofisica e Vulcanologia, Rome, Italy
[4]Institute of Education, Research and Regional Cooperation for Crisis Management Shikoku, Kagawa University, Takamatsu, 760-8521, Japan

Correspondence to: Hafize Başak Bayraktar (hafizebasak.bayraktar@unina.it)

Abstract. In this study, time-dependent probabilistic tsunami hazard analysis (PTHA) is performed for Tuzla, Istanbul in the Sea of Marmara, Turkey, using various earthquake scenarios of Prince Island Fault (PIF) within next 50 and 100 years. Monte Carlo (MC) simulation technique is used to generate a synthetic earthquake catalogue, which includes earthquakes having moment magnitudes between M_w 6.5 and 7.1. This interval defines the minimum and maximum magnitudes for the fault in the case of entire fault rupture, which depends on the characteristic fault model. Based on this catalogue, probability of occurrence and associated tsunami wave heights are calculated for each event. The study associates the probabilistic approach with tsunami numerical modelling. Tsunami numerical code NAMI DANCE was used for tsunami simulations. According to the results of the analysis, distribution of probability of occurrence corresponding to tsunami hydrodynamic parameters are represented. Maximum positive and negative wave amplitudes show that tsunami wave heights up to 1 m have 65% probability of exceedance for next 50 years and this value increases by 85% in Tuzla region for the next 100 years. Inundation depth also exceeds 1m in the region with probabilities of occurrence of 60% and 80% for the next 50 and 100 years, respectively. Moreover, probabilistic inundations maps are generated to investigate inundated zones and the amount of water penetrated inland. Probability of exceedance of 0.3 m wave height ranges between 10% and 75% according to these probabilistic inundation maps and the maximum inundation distance calculated among entire earthquake catalogue is 60 m in this test site. Furthermore, synthetic gauge points are selected along the western coast of the Istanbul by including Tuzla coasts. Tuzla is one of the areas that show high probability exceedance of 0.3 m wave height, which is around 90%, for the next 50 years while this probability reaches up to more than 95% for the next 100 years.

1 Introduction

Marmara region, especially highly populated cities along the coasts of the Marmara Sea, is the heart of Turkish economy in terms of having great number of industrial facilities in largest capacity and potential, refineries, ports and harbors. The Marmara Sea and the area is one of the most seismically active areas in Turkey. Main active faults of the region pass through the

Marmara Sea. Thus, coastal cities in Marmara region, especially Istanbul, which has significant importance in terms of economy, and historical and sociocultural heritage with a population of more than 15 million, is under the threat of high damage due to possible big earthquake and also triggered tsunamis. Recent studies and evaluation of earthquake recurrence periods

35 revealed that there is a high possibility of having an earthquake with magnitude larger than M_w 7.0 in PIF. According to Ambraseys (2002), the latest earthquake on this fault system occurred in 1766 and since that time, this fault has been accumulating huge amount of energy. According to Parsons (2004), the probability of occurrence of M>7 earthquake beneath the Marmara Sea was estimated to be 35-70% in the following 30 years. The region has distinctive characteristics in terms of its complex tectonic structure and high possibility of an earthquake occurrence with the magnitude larger than 7.0 offshore

40 Istanbul mega-city. Therefore, there has been a wide range of studies in Marmara Sea region regarding the fault mechanisms, seismic activities, earthquakes and triggered tsunamis (Armijo et al., 2002; Armijo et al., 2005; Okay et al., 1999; Le Pichon et al., 2001; Yaltirak 2002; McNeill et al., 2004; Aksu et al., 2000; Imren et al., 2001; Pondard et al., 2007, Yalçıner et al., 1999; Yalçıner et al., 2000; Yalçıner et al., 2002; Aytore et al., 2016 ; Hebert et al., 2005; Altınok et al., 2003; Altınok et al., 2011; Guler et al., 2015; Cankaya et al., 2016; Tufekci et al., 2018; Latcharote et al., 2016).

45 The North Anatolian Fault Zone (NAFZ) controls the great part of the seismic activity in the Marmara Sea region. The fault zone sets apart Anatolia (Asian part of Turkey) and Eurasia due to the northward migration of Arabian Plate in the east and southward rollback of the Hellenic subduction zone in the west as seen in Fig. 1 (Armijo et al., 1999; Flerit et al., 2004; Le Pichon et al., 2015).
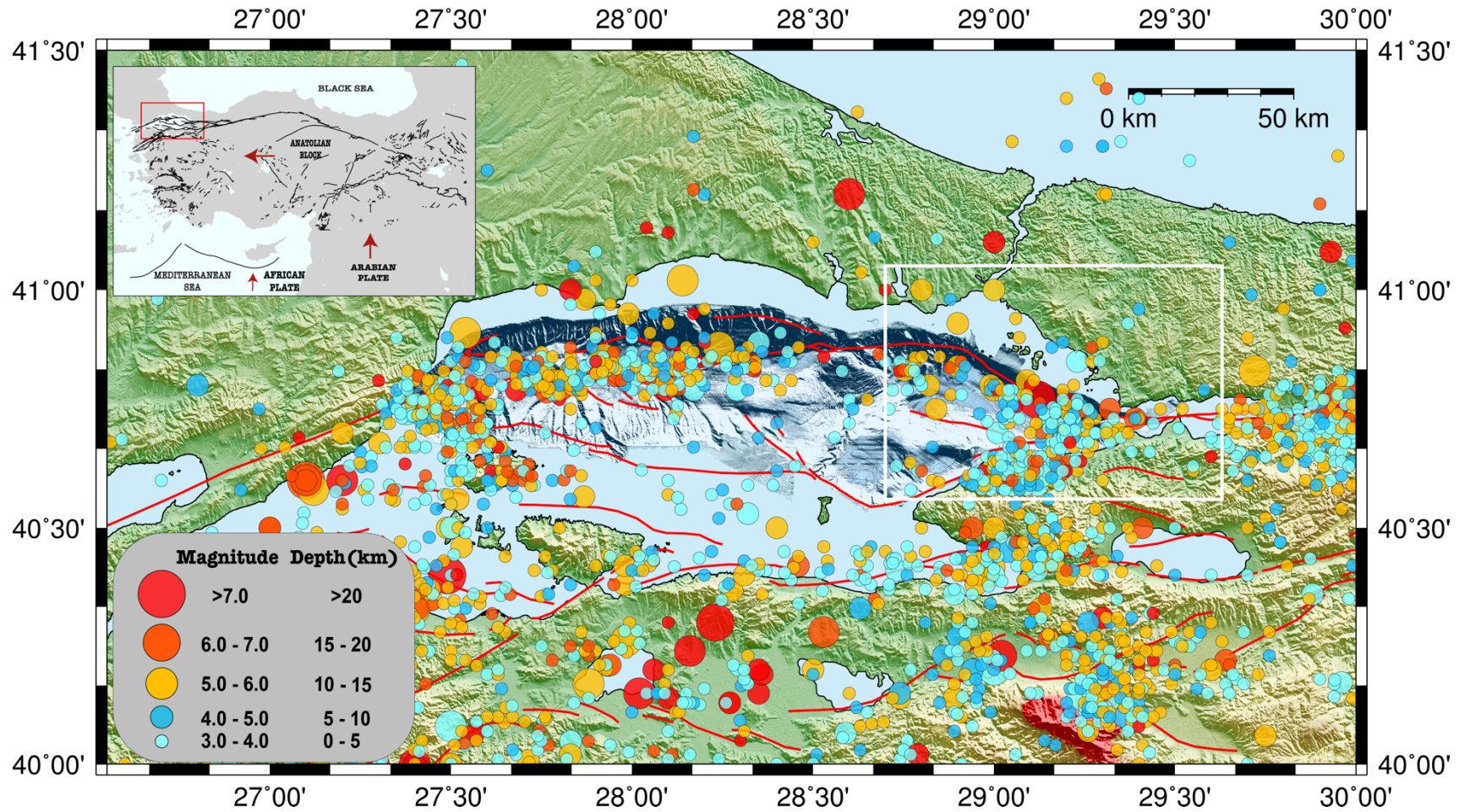
Figure 1: Seismicity map of the Marmara region and general tectonic map of the Turkey on the top – left. In the seismicity map, the size of the circle's changes with magnitude of the earthquakes and the color of the circles defines the depth change of the earthquakes. Red lines show the known active faults (Modified from Emre et al., 2013) in the region and white square is the area with the PIF. In the general tectonic map of Turkey, red arrows show the direction of the plate motion, black lines show the active faults in the region (Modified from Emre et al., 2013) and red rectangular shows the Marmara region (created using The Generic Mapping Tools, Version 5.4.1).

55   The Marmara Sea region is a transition zone between the strike-slip regime of the NAFZ and the extension regime of the Aegean Sea area (on the top – left of Fig 1). The northern branch of the NAFZ forms a major transtensional NW- SE right bend under the Sea of Marmara at Çınarcık trough (Murru et al., 2016). The fault trace is attached to the complex Central Marmara and Tekirdağ pull-apart basins, before joining the NE-SW striking Ganos fault on land by following the northern margin of the Marmara Sea. Finally, the fault exits into the Aegean Sea by way of Saros Gulf (Wong et al., 1995; Armijo et

60   al., 1999; Armijo et al., 2002; Okay et al., 1999; Le Pichon et al., 2001; Yaltirak 2002; McNeill et al., 2004). The fault trace beneath the Marmara Sea is not directly observable. Therefore, making a segmentation model for the offshore parts of the NAFZ is quite challenging, which causes the fault dimensions, such as its length and width, to include a sum of error margin (Aksu et al., 2000; Imren et al., 2001; Le Pichon et al., 2001; Armijo et al., 2002; Armijo et al., 2005; Pondard et al., 2007). The current right-lateral slip rate along the NAFZ is about 25 mm/yr (Meade et al., 2002; Reilinger et al., 2006). In the western

65   side, the motion between the Anatolia and Eurasia plates is accommodated across the Marmara region by ~ 19 mm/yr of right-lateral slip and 8 mm/yr of extension (Flerit et al., 2003; Flerit et al., 2004). Slip rates of the main Marmara fault ranges between 17-28 mm/yr (Le Pichon et al., 2003; Reilinger et al., 2006). On the other hand, Hergert and Heidbach (2010) suggests that the right-lateral slip rate on the main Marmara fault is between 12.8-17.8 mm/yr due to slip partitioning and internal deformation. The right-lateral slip rate for the PIF and Çınarcık basin is 15±2 mm/yr and in addition to this, the fault has 6±2 mm/yr of

70   extension (Ergintav et al., 2014).

     The main characteristic of the NAFZ is having earthquakes systematically propagated westward and historical records show that, northern strand of the NAFZ generates an earthquake with the recurrence interval of about 250 years beneath the Marmara Sea and the latest event occurred in 1766 (Ambraseys, 2002, Bohnhoff et al., 2013). This event caused the rupture of the 58 km long northern part of NAFZ from Izmit to Tekirdağ (Ambraseys and Finkel, 1995; Ambraseys and Jackson, 2000).

75   However, the earthquake that happened on 2 September 1754 can be considered as the latest characteristic event for the PIF segment and it caused the rupture of a 36 km long fault segment (Ambraseys and Jackson, 2000). The NAFZ has experienced two M>7 earthquakes in August 1912 Ganos and August 1999 Izmit earthquakes recently. After the 1999 Izmit event, seismic energy along the 150 km long northern part of the NAFZ has been accumulating continuously since 22 May 1766 earthquake. This fault zone extends right next to south of Istanbul beneath the Marmara Sea, and this situation increases the rupture

80   possibility of the PIF and the risk for megacity Istanbul (Stein et al., 1997; Barka 1999; Bohnhoff et al., 2013). Ergintav et al., (2014) also indicated that the PIF segment accumulates stress 15±2 mm/yr and the 3.7m slip deficit has been accumulating since the 1766 events and this makes PIF most likely to generate the next M > 7 earthquake along the Sea of Marmara segment of the NAF.

     Beside these seismic activities in the region, studies on the historical tsunami records show that 35 tsunami events happened

85   between BC 330 and 1999 in the Marmara Sea region and the majority of them are earthquake-related tsunami events (Altinok et al., 2011; Yalçıner et al., 2002). The 1509 earthquake, with an estimated magnitude around 7.5 (Ambraseys, 2002), is one of the examples for these events. This earthquake triggered a tsunami and the tsunami waves inundated along Istanbul coasts, reaching the city walls and around 4000–5000 people died in the city (Ambraseys and Finkel, 1995). The 1894 earthquake is

also one of the important events that happened in the Marmara Sea. The earthquake triggered a tsunami and the sea inundated 200 m in Istanbul (Altinok et al., 2011). The recent one happened after the 17 August 1999 Izmit earthquake and after the earthquake, E-W trending tectonic deformation along the basin and submarine failures generated a tsunami. The International Tsunami Survey Team (Yalçıner et al., 1999; Yalçıner et al., 2000) investigated the region and they observed 2.66 m run-up along the coast from Tütünçiftlik to Hereke and 2.9 m run-up at Değirmendere (Yalçıner et al., 2002).

Several tsunami hazard estimation studies (Ozer Sozdinler et al., 2020; Hancilar, 2012; Aytore et al., 2016; Hebert et al., 2005) were also conducted in the region. These tsunami analyses were mostly performed in deterministic manner using various earthquake scenarios depending on the combinations of different fault parameters without considering probability of occurrences. The 40 km long fault in Eastern Basin of Marmara Sea, with a significant normal component, may generate tsunami wave which can reach maximum 2 m height along the Istanbul coast with locally considerable inundation (Hebert et al., 2005). The rupture of Yalova Fault, PIF or Central Marmara Fault can also cause a serious damage along the coast of Istanbul. Tsunami wave heights can reach 4.8m and can penetrate 340m inwards from the coast in Haydarpaşa Port (Aytore et al., 2016).

A few probabilistic seismic and tsunami hazard analyses (Murru et al., 2016; Erdik et al., 2004; Hancilar, 2012) were also done in this region. Seismic hazard maps were prepared in the Marmara Sea region by describing fault segments and peak ground accelerations with the periods corresponding to 10% and 2% probabilities of exceedance in 50 years (Erdik et al., 2004). Besides that, tsunami inundation maps are prepared based on probabilistic and deterministic analyses by depending on these segmentations (Hancilar, 2012). Time-dependent and time-independent earthquake ruptures are also estimated in the Marmara Sea region for the next 30 years (Murru et al., 2016). These previous studies have been conducted for entire Marmara Sea region and therefore they give general and rough information about probability of occurrence in the region without focusing on any specific region in high resolution. However, probabilistic tsunami hazard assessment is important to calculate the tsunami exposure and risk on human populations and infrastructures, since probability calculations consider all possible earthquakes in a fault even if they occur with very low probability (Løvholt et al., 2012; Løvholt et al., 2015; Grezio et al., 2017). The results of probabilistic studies should be considered when decision makers design coastal zones and structures, especially critical ones. Different from previous probabilistic approaches in the Marmara Sea, the probability of earthquake occurrences in one fault segment, PIF, are taken into account for the preparation of high-resolution tsunami inundation maps and distribution of hydrodynamic parameters due to the probability of occurrence of associated earthquakes on PIF determined by MC Simulations.

This PTHA study depends on the fully characteristic fault model and the main purpose is to perform PTHA for selected test site. Tuzla test site is one of the coastal districts of Istanbul and located on the southernmost part of the city (Fig 2). The region includes several residential areas, but the most critical point about the region is that Tuzla has the biggest shipyard area not only in the Marmara Sea but also in Turkey (Fig 3). In this study we mainly focused on this region because it is about 20km away from the PIF and therefore has high risk of both earthquake and tsunami damage.
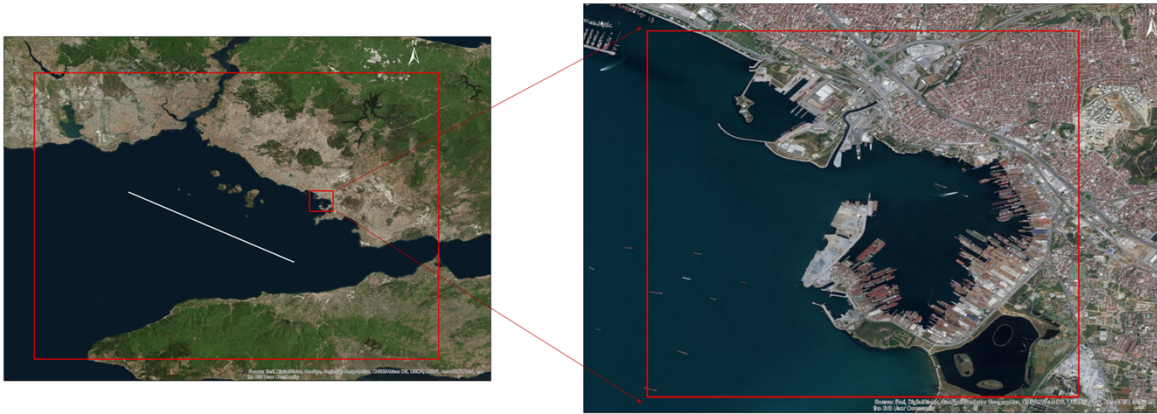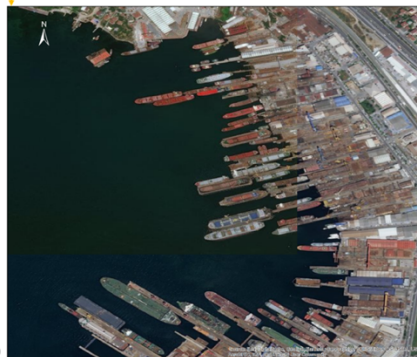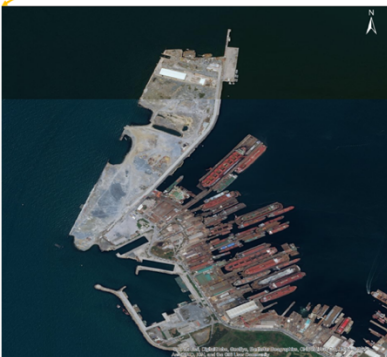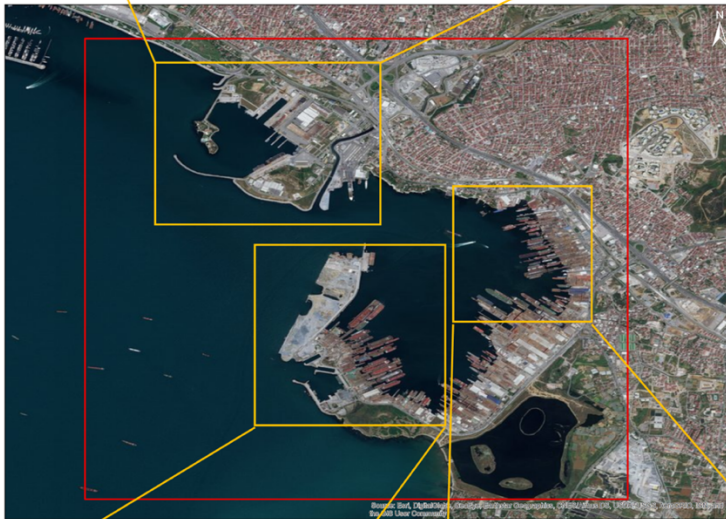
Figure 2: The Marmara Sea Region, Tuzla Test Site and the Location of PIF Segment which is used in the analysis like a straight line (created using ArcMap Version 10.5).

Figure 3: Some Important Locations at Tuzla Domain (a)Northern part of the Tuzla domain. (b) Southern part of the Tuzla Domain. (c) Tuzla Shipyard (created using ArcMap Version 10.5).

125

2 Probabilistic Analysis

Probabilistic tsunami hazard analysis (PTHA), as it is recently becoming a widely-used procedure for coastal zones, is
130 performed for Tuzla region, Istanbul. This method has been applied for various tsunami sources, such as earthquakes, landslides, volcanic activities etc. in various scales, local, regional and global (Grezio et al., 2017). For the earthquake generated tsunamis, the method is generally adapted from seismic hazard assessment methods (González et al., 2009). Such kind of studies consider the events that are generated by co-seismic sea floor displacement, Seismic Probabilistic Hazard Analysis (SPTHA), but numerous tsunami simulations are required to consider all expected combination of seismic sources.
135 This problem can be solved by applying a simplified event tree approach and a two-stage filtering procedure to reduce the number of required source scenarios without decreasing the quality and accuracy of inundation maps (Lorito et al., 2015). The earthquake source itself is very uncertain and the investigation of this uncertainty can be done by building an event tree instead of using logic tree and hazard integrals (Selva et al., 2016). Logic tree approach can be applied to generation of tsunami hazard curves to decrease the uncertainties by including branches, which are the combination of tsunami sources, magnitude
140 distribution of characteristic tsunamigenic earthquakes, their recurrence interval, and tsunami height estimation procedure based on a numerical simulation (Annaka et al., 2007). For regional studies, hazard curves can be generated by empirical analysis using available tsunami run-up data. However, if such data is not available, MC simulations, a computational based method widely used in probabilistic seismic hazard analysis (PSHA), can be considered as a primary method to generate tsunami hazard curves (Geist and Parsons, 2006; Horspool et al., 2014). Submarine landslides, on the other hand, are the major
145 tsunami source for passive margins, which are the transition zone between oceanic and continental lithosphere that is not an active plate boundary, and they have been included in PTHA methodologies (Geist and Lynett, 2014). Probabilistic studies are also applied to develop multi – hazard loss estimation methodology for coastal regions that are exposed to cascading shaking-tsunami hazards due to offshore mega-thrust subduction earthquakes (Goda and Risi, 2018).

In this study, characteristic earthquake model is used to estimate the earthquake recurrence on PIF. Paleoseismologic studies
150 (Ryall et al., 1966; Allen, 1968; Schwartz and Coppersmith, 1984) suggest that an individual fault tends to generate characteristic earthquakes having a very narrow range of magnitudes. These individual faults have a different frequency distribution than the log linear Gutenberg-Richter frequency-magnitude relationship (Aki, 1984; Schwartz and Coppersmith, 1984; Youngs and Coppersmith, 1985). According to Aki (1984), characteristic earthquake is generated as a result of constancy of barriers to rupture through repeated seismic cycles.

155 PIF is fully characteristic and a characteristic earthquake will rupture entire fault as a whole and release the entire energy. Therefore, while performing MC simulations, area of the fault and fault parameters (strike, dip and rake angles) are used as constants referring to the outcomes of EU 7th Frame Project MARSITE (Ozer Sozdinler et al., 2020). One of the work packages of this project aimed to define the geometry of the possible tsunamigenic faults in the Marmara Sea and 30 different earthquake scenarios with the different rupture combinations of 32 possible fault segments. Based on these 30 different earthquake
160 scenarios, tsunami numerical modelling is performed. The definition of fault segments depends on extensive review of the

literature (Alpar and Yaltırak, 2002; Altınok and Alpar, 2006; Armijo et al., 2005; Ergintav et al., 2014; Gasperini et al., 2011; Hebert et al., 2005; Hergert et al., 2011; Hergert and Heidbach, 2010; Imren et al., 2001; Kaneko, 2009; Le Pichon et al., 2001; Le Pichon et al., 2003; Le Pichon et al., 2014; Oglesby and Mai, 2012; Sengor et al.,2014; Tinti et al., 2006; Utkucu et al., 2009). As a result of this review, each fault segment is defined as a rectangular area with hypothetical uniform slip. According to the results of the project, the fault parameters of the PIF, are given in Table 1. The 3D Fault configuration given by Armijo et al., 2002, which explains fault segmentation in the region depending on morphology, geology and long-term displacement fields, also fits with the PIF parameters that are used in the project. These parameters are used as constants in this study while assessing probability of occurrence of each earthquake to allow entire fault rupture at different depths with different magnitudes.

Fault Length (km)	Fault Width (km)	Strike	Dip	Rake
33.5	14	119	80	210

Table 1: The area and the focal mechanism of the PIF zone. These are the constant parameters during the MC simulation application.

MC simulation technique is generally applied to generate earthquake catalogue of a given length of time. In this technique, a list of earthquakes can be generated using the frequency - magnitude relationship for each seismic source (Zolfaghari, 2015). Seismic zonation should be done by considering regions that have relatively homogeneous earthquake activity and faulting regimes (Sørensen et al., 2012). In this study, fault segment model proposed in Ozer Sozdinler et al., 2020 is used and PIF is the only segment for seismic source. After that, tsunami numerical modelling is performed for each event of this synthetic catalogue and tsunami hydrodynamic parameters, mainly maximum wave heights, inundation depth, current velocities, as well as tsunami inundation zones are estimated. Tsunami risk assessment will serve the best for the needs of societies when associate regional studies with the local ones (Sørensen et al., 2012).

MC simulation technique allows generating a list of earthquakes based on a frequency-magnitude relationship. This technique depends on a uniformly distributed source model and it provides equal chance to each earthquake source. As a result, synthetic earthquake catalogue will have uniformly random distributed earthquake sources (Zolfaghari, 2015).

Using MC simulation, a synthetic earthquake catalogue is generated by selecting earthquake magnitude and depth as uniformly distributed random numbers in a given interval and using area and directivity of the fault as a constant variable (Table 1). We performed MC simulations 100 times for having 100 different earthquake scenarios. The number of earthquakes in the catalog is selected as a reasonable number, which represents the number of iterations randomly done in MC simulations for having a synthetic earthquake scenario. As mentioned earlier, NAFZ generates an earthquake with the recurrence interval of about 250 years beneath the Marmara Sea. Therefore, selecting 100 earthquake scenarios would cover a time period of 100x250 years= 25,000 years which is considered as an adequate catalog duration in this study. However, because of having time dependent

probabilistic analyses, this catalog duration is not used for PTHA in this study.

Earthquake magnitude is one of the parameters randomly selected by the MC technique. Based on a characteristic earthquake model, individual faults tend to rupture entire fault when a large earthquake occurred. This model assumes that characteristic earthquake releases all of the seismic energy during the fault rupture and the magnitude of the earthquake depends on the dimension of fault (Abrahamson and Bommer, 2005).

As mentioned previously, only the PIF is considered as an earthquake source with approximately 34 km in length and 14 km in width (Ozer Sozdinler et al., 2020; Karabulut et al., 2002). This fault zone is assumed that it has potential to generate a characteristic earthquake and rupture the entire fault. According to Wells and Coppersmith (1994) scaling relation between fault area and magnitude (Eq. 1), this fault can generate a characteristic earthquake with the magnitude varying between M_w 6.5-7.1.

$$M_w = a + b * \log (L * W) \tag{1}$$

In this equation, a and b are coefficient, which are 4.33 and 0.9 respectively, L is fault length and W is the fault width.

Displacement on the fault surface calculations are done, for each randomly selected magnitude, using the formulation of Aki (1966),

$$D = \frac{M_o}{\mu A} = \frac{10^{(M_w+6.07)*1.5}}{\mu A} \tag{2}$$

where D is displacement on the fault surface, M_w is moment magnitude, μ is the shear modulus (μ=30 GPa), and A is the fault area.

Seismogenic thickness and the location of the earthquake is another important parameter required for earthquake and tsunami source. At first, the PIF zone is accepted as fully characteristic and an earthquake should rupture the entire fault area. Therefore, it is assumed that if the rupture starts at the center of the fault and continues in both directions, the fault will rupture entirely. For this reason, the locations of the earthquakes are accepted as the midpoint of PIF zone for each earthquake scenario (Ozer Sozdinler et al., 2020).

For the seismogenic thickness, the seismic activity of the northern segment of NAFZ starts at the depth of 5 km (Karabulut et al., 2003). The bottom of the seismogenic thickness can be determined based on the after-shock activity of the 17 August 1999 Izmit Earthquake. The earthquakes on the northern scarp of the Çınarcık basin are observed between the depths of 5 and 14 km. The mechanism of events between the depth of 5 and 10 km shows the behavior of normal faulting. On the other hand, strike-slip mechanism dominates the depths below 10 km to 14 km. As a result, seismic activity can be observed between the depths of 5-14 km and fault plane solutions show normal and strike-slip mechanisms in this area (Karabulut et al., 2002). Therefore, depth of events vary between 5 to 14 km in MC simulations.

In time - independent earthquake occurrence models, probability of an event occurrence follows a Poisson distribution in a given certain period of time. Therefore, the result of this model does not vary in time. However, probability of an earthquake occurrence is based on the time that has passed since the occurrence of last event and it follows a Brownian passage time (BPT), log-normal or another probability distribution (Matthews et al., 2002; Ellsworth et al., 1999; Davis et al., 1989; Rikitake

225   1974). In this model, in addition to the recurrence time of earthquake, variability of the frequency of events and the elapsed time from the last characteristic event are the additional required information and the longer elapsed time causes to increase of probability of an event occurrence (Cramer et al., 2000; Petersen et al., 2007).

Calculation of probability in multi – segment ruptures and more complicated models includes Gutenberg Richter magnitude – frequency relationship (Gutenberg and Richter, 1944). The application of time – dependent models based on characteristic

230   earthquake model, which assumes all large events occurring along a particular fault segment would have similar magnitudes, rupture area and average displacements (Schwartz and Coppersmith, 1984). Therefore, this model is suitable for calculating the probability of occurrence of an earthquake on a single fault.

It should be noted that, in this study, PIF is considered as the only source for the earthquake and tsunami. Time dependent probabilistic model is followed for the probability calculations; because, this probabilistic model allows to consider only one

235   fault instead of using multi – segment rupture scenarios through characteristic earthquake model.

In the time-dependent approach, BPT probability model is used to obtain the recurrence time probability of the earthquake in the fault segment. This model does not show significant difference with the log – normal distribution except for consideration of very long elapsed times from the last characteristic event (Petersen et al., 2007). A characteristic event occur when the load-state process reaches to the failure threshold; an earthquake releases all energy loaded on the fault and then starts the new

240   failure cycle. The time interval between consecutive earthquakes shows a Brownian passage time distribution and that can be useful to forecast long term seismic events by generating a time – dependent model (Matthews et al., 2002). The Working Group on California Earthquake Probabilities (1999) and the Earthquake Research Committee (2001) have already implemented this time – dependent approach to the San Francisco Bay and Japan, respectively, for the prediction of long-term events (Petersen et al., 2007). This model depends on the time period passed since the last characteristic event and recurrence

245   time of the earthquake. The probability density function for BPT model (Matthews et al., 2002) is given by,

$$f(t, T_r, \propto) = (\frac{T_r}{2\pi\alpha^2 t^3})^{1/2} \exp (\frac{(t-T_r)^{1/2}}{2T_r\alpha^2 t}) \tag{3}$$

where t is the elapsed time from the last characteristic event and α is the aperiodicity (also known as the coefficient of variation). Aperiodicity defines the regularity of the expected characteristic earthquakes on the fault and varies between the 0.3 and 0.7. This parameter, which is known as the parameter defining how much an expected characteristic earthquake occurs

250   regularly or irregularly on any fault segment (Murru et al., 2016), was taken as 0.5 in this study (Parsons, 2004). The mean recurrence interval of earthquakes (T_r) can be defined as the ratio between the mean moment of repeating earthquakes (seismic moment) and the long-term moment accumulation rate on the fault (moment rate) (Ren and Zhang, 2013). Seismic moment can be obtained using the formulation of Kanamori (2004) and the moment rate of the fault is calculated from fault area and long-term slip rate of the fault (WGCEP 2003).

255    $$T_r = \frac{M_o}{\dot{M_o}} = \frac{10^{(M_w+6.07)*1.5}}{\mu V A} \tag{4}$$

In this equation, M_w is moment magnitude, μ is the shear modulus, V is long-term slip rate in mm/yr and A is the fault area. The moment magnitude value in Eq. (4) was selected randomly using MC simulations. Thus, seismic moment (M_o) and the

mean recurrence time (T_r) were calculated for each earthquake scenario. Long term slip rate is also selected as 17 mm/yr for this equation (Ergintav et al., 2014).

260 Probability of the earthquake occurrence on the fault is calculated based on the probability density function approach. The probability of occurrence of an event in the next ΔT years, given that it has not occurred in the last t years is given by (Erdik et al., 2004),

$$P(t, \Delta T) = \frac{\int_t^{t+\Delta T} f(t)dt}{\int_t^{t+\infty} f(t)dt} \tag{5}$$

In this case, probability of a characteristic earthquake was calculated using ΔT as 50 and 100 years.

265 **3 Tsunami Numerical Modelling**

Tsunami simulations are performed for each earthquake in synthetic catalogue using tsunami numerical model NAMI DANCE (NAMI DANCE, 2011). The code is the user-friendly version of TUNAMI-N2 (Imamura et al., 2001) developed in C++ language, which computes all fundamental parameters of tsunami motion in shallow water and in the inundation zone. It uses explicit numerical solution of shallow water wave equations with finite-difference technique and allows for better

270 understanding of the effect of the tsunami waves (Shuto et al., 1990; Imamura, 1989). NAMI DANCE can solve both Linear and Nonlinear Shallow Water (NSW) Equations with selected coordinate system (Cartesian or spherical) and calculates the tsunami motion. LSW equations are preferable in deep water because of reasonable computer time and memory and calculates the results in acceptable error limit (Insel, 2009). NAMI DANCE is validated and verified using NOAA standards and criteria for tsunami currents and inundation (Synolakis et al., 2007; Synolakis et al., 2008). The numerical solutions of NAMI DANCE

275 are also tested, validated and verified against analytical solutions, laboratory measurements and field observations (NTHMP, 2015; Lynett et al., 2017; Velioglu, 2009).

NAMI DANCE calculates tsunami generation using Okada (1985) equations. In this study, water surface distribution of tsunami source (initial wave amplitude) are calculated with this method for 100 earthquakes of the synthetic earthquake catalogue prepared by MC simulations. As an example, Figure 5 shows the initial water surface calculated due to one of 100

280 tsunami sources generated by MC simulations (Fig 5).

Before starting tsunami simulations, the necessary inputs should be prepared precisely in order to obtain reliable results. Bathymetry - topography data is one of the most important input in NAMI DANCE that significantly effects the reliability of results especially in shallow water zone due to the nature of NSW Equations. NAMI DANCE can make nested analyses under the condition that grid size of study domains have a certain 1:3 ratio between each other. Therefore, we generated four nested

285 domains having the coarsest grid size as 81 m and the finest grid size as 3 m with 1:3 ratio in GIS environment. Bathymetric data for the biggest domain is the combination of 30 arc second resolution General Bathymetric Chart of the Oceans (GEBCO) and data produced by navigational charts in shallow zones. Topographic data, on the other hand, contains the high resolution, which is obtained from the Department of Housing and Urban Development of Istanbul Metropolitan Municipality, Digital Elevation Model (DEM) and vector data with resolution 5m and 1m, respectively. The bathymetry - topography data in the

290 smaller domains is the downscaled version of the 81m grid sized bathymetry-topography data, however high resolution digitized coastline, and sea and land structures are also included to the data to generate 3m grid sized smallest domain (Fig 4). Synthetic gauge point file is another required input of the NAMI DANCE. In addition to the calculation of principal tsunami hydrodynamic parameters, program can also calculate the change of water level, current velocity and flow depth over time in every gauge point. Therefore, various gauge points are selected along the coast of nested domains, near shore and offshore and
295 close to some critical structures on land.

During the inundation of tsunami waves, current velocity is an important tsunami parameter in land and sea, especially in ports and bays. Strong current velocities may cause dragging offshore or landing of sea vessels inland. This parameter as well as tsunami wave amplitude, inundation depth and Froude number can be calculated by NAMI DANCE. However, in this study, the results are represented based on only the probability of exceedance of threshold values for water surface elevation and
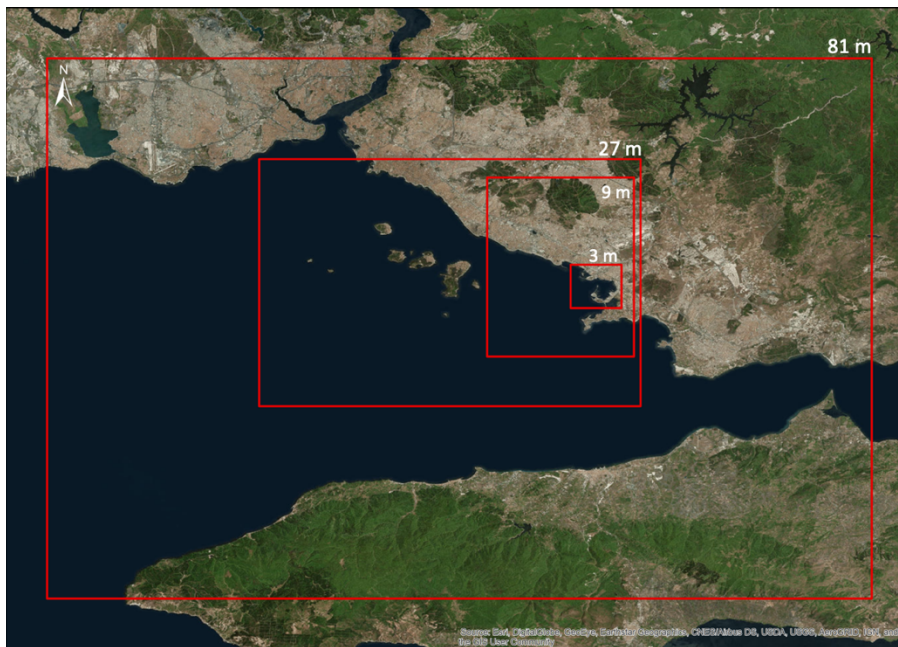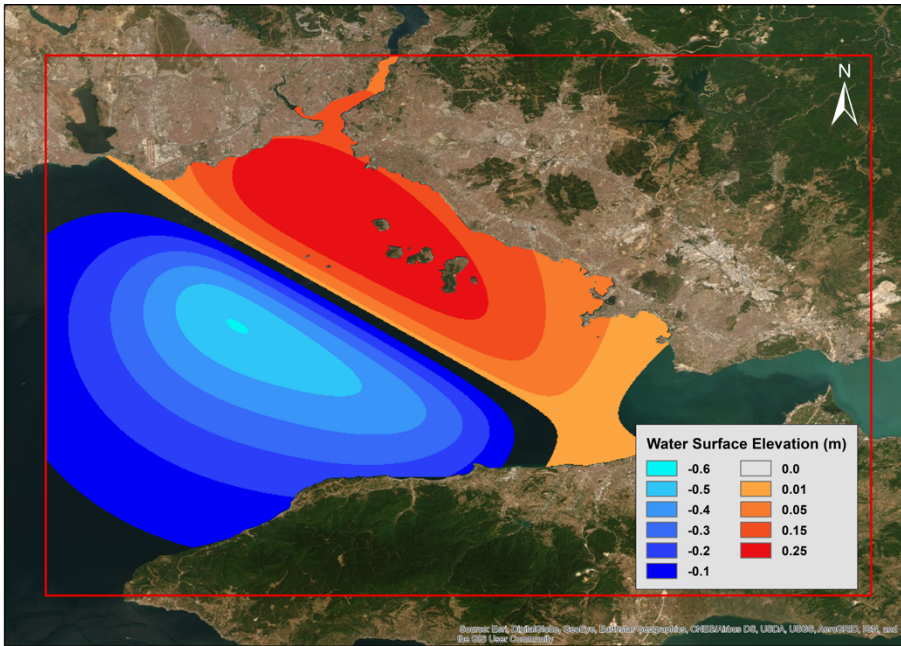300 inundation depth.

Figure 4: Nested domains for tsunami numerical modelling. Red rectangles show the limits of these domains. Grid size of these domains have a certain 1:3 ratio between each other (created using ArcMap Version 10.5).

13

305 **Figure 5: Initial water surface distribution of one of the 100 tsunami sources. Red frame indicates the boundary of largest nested domain with 81m grid size (plotted using ArcMap Version 10.5).**

4 Results and Discussion

In this study, tsunami hydrodynamic parameters are calculated in both coarsest domain (whole Marmara Sea) and finest domain
310 (Tuzla region). The main parameters focused in this study are the tsunami wave heights and inundation depths and the results are shown in the terms of probability of exceedance of threshold wave height and inundation depth values within the next 50 and 100 years. The situation for the next 500 years is not considered because the return period of the fault rupture is about 250 years, which means this fault generates at least one earthquake within the next 500 years. In other words, probability of exceedance for the next 500 years will be about 99%.

315 We present the results of the PTHA for Tuzla test site in terms of three different visualization categories for the next 50 and 100 years. First, distribution of probability of occurrence of the tsunami hydrodynamic parameters, which are minimum and maximum water surface elevation and inundation depth, are shown. Second, tsunami inundation maps that show probability of exceedance of 0.3 m inundation depth for different time periods are generated for Tuzla region in order to observe flooded areas and their probabilities clearly. And finally, the probability map of exceedance of 0.3 m wave heights at synthetic gauge
320 points are represented as bar charts.

4.1 Probability of Exceedance for Entire Synthetic Earthquake Catalogue

The graphics are generated to demonstrate the probabilities of occurrences corresponding to the minimum and maximum water surface elevations and inundation depth calculated from tsunami sources of each earthquake in synthetic earthquake catalogue. It should be noted that in case of having same magnitude of earthquakes in two different earthquake scenarios of the catalogue,

14

the probability of occurrences of these scenarios would be the same. However, since they would have different focal depths, the tsunami initial wave height calculated by Okada (1985) will be different, which results in the calculation of different hydrodynamic parameters. As a result, the graphs show different maximum water surface elevations having the same probability of occurrences.

In Figure 6, graphics of probabilities of occurrences according to maximum and minimum water surface elevation (maximum water withdraw) and inundation depth for next 50 years are represented, respectively. According to these graphs, tsunami wave heights up to 1 m and withdrawal of the waves around 1 m have approximately 65%±15 probability of occurrence. Tuzla region includes various shipyards, ports and other important facilities. Therefore, probability of the withdrawal of the water is as important as maximum water surface elevation. 1 m height of wave withdrawal may cause the ships to be stranded at the ports and results in extreme financial losses as observed in the 20th July 2017 Bodrum-Kos earthquake and tsunami (Yalçıner et al., 2017). The probability for having 1 m inundation depth, on the other hand, can be predicted as about 60%±10. Residual of probability with respect to the fitted curve for each data point is demonstrated right after the percentage of probability with ± sign.
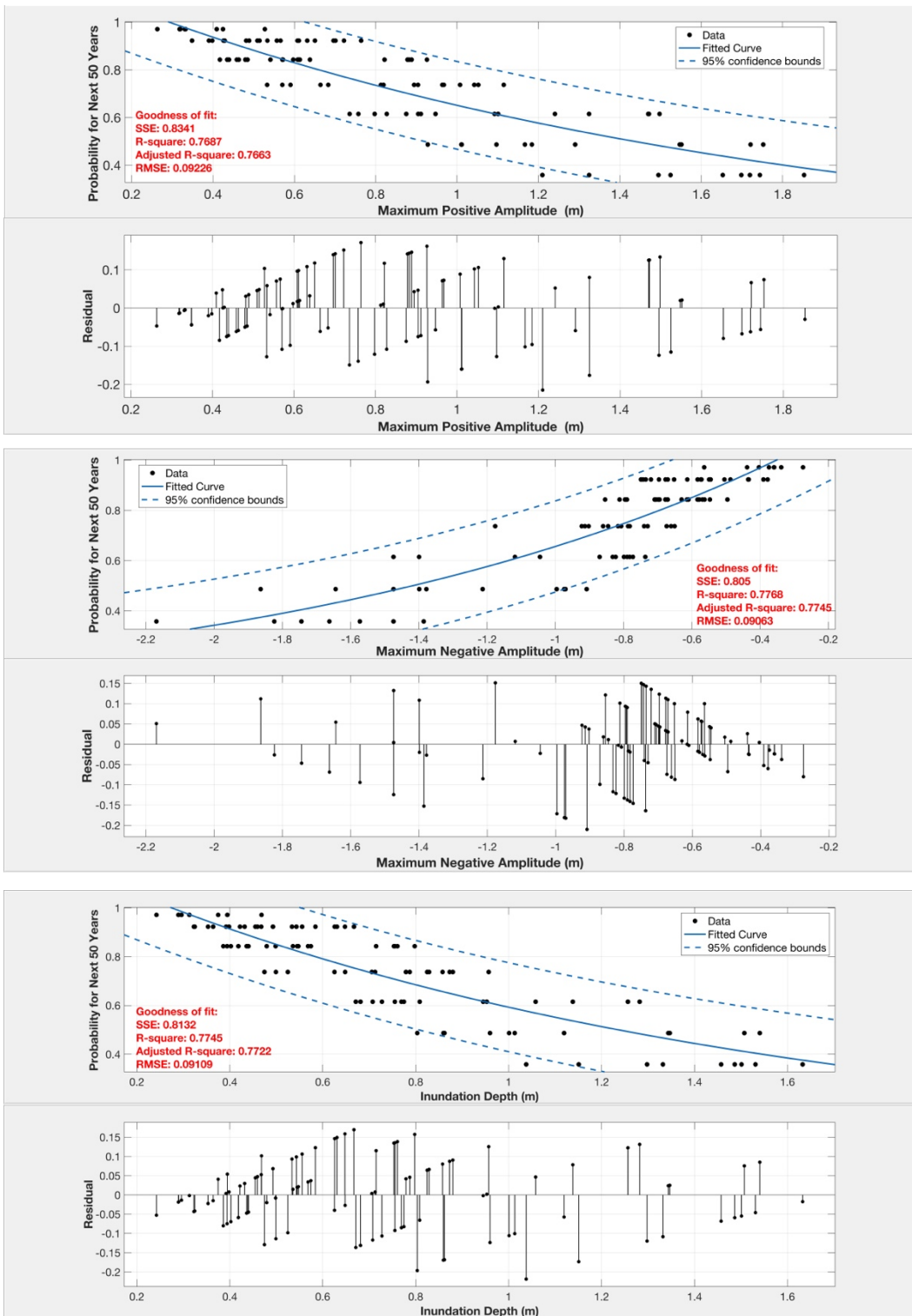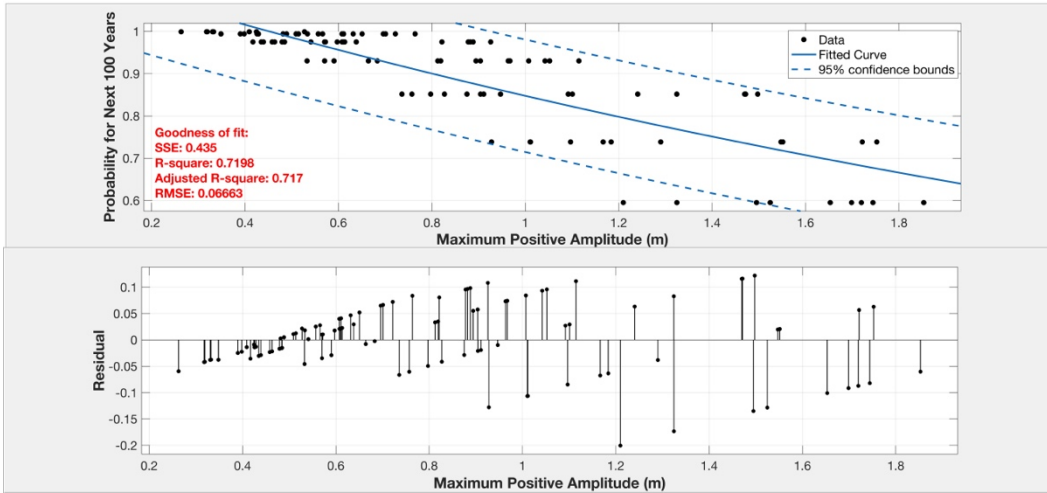
340

Figure 6: Probabilities of Exceedance Corresponding to Maximum Water Surface Elevation, Minimum Water Surface
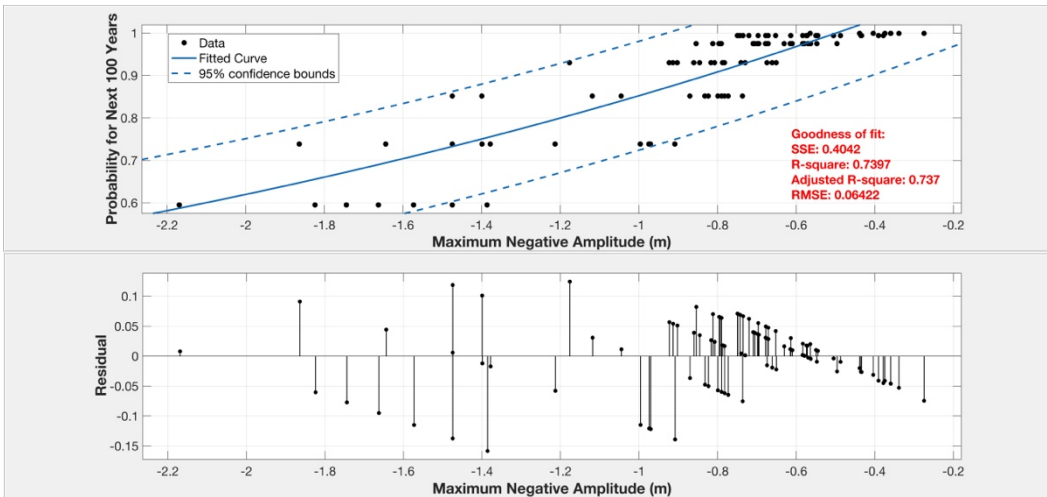
Elevation and Inundation Depth for the next 50 years. Black dots represent the probability of exceedance of tsunami hydrodynamic parameter for each event in the catalog. Blue line is the best fit curve to the data and dashed blue line is the 95% confidence boundary of the fitted curve. Residual of the fit is represented for each probability curve.

345

The situation for next 100-years (Fig 7) obviously shows that probability of occurrences would increase with time. The probability of exceedance of 1 m water surface elevation and 1 m wave withdrawal reaches up to 85%±10. Probability of exceedance of inundation depth also changes significantly. The probability of exceedance of 1 m inundation depth is found around 80%±10.
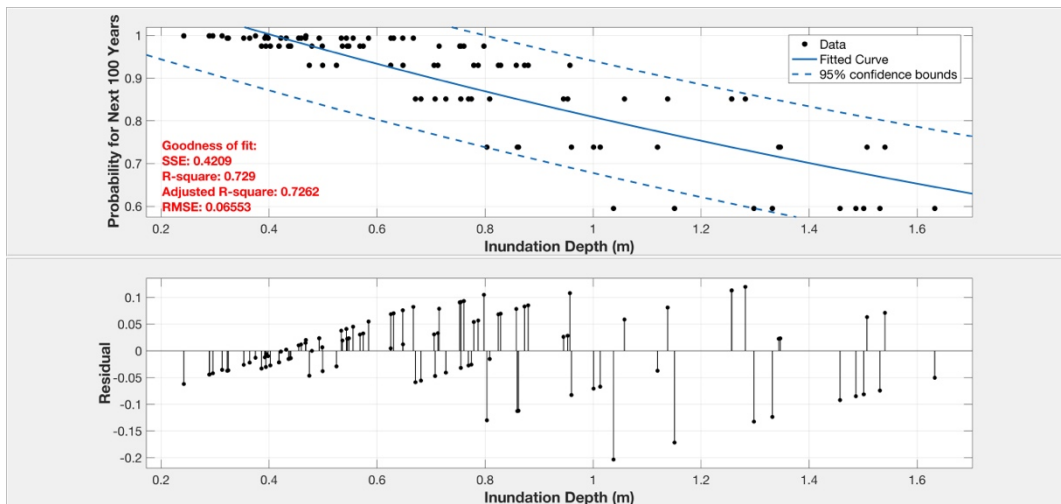

350

Figure 7: Probabilities of Exceedance Corresponding to Maximum Water Surface Elevation, Minimum Water Surface Elevation and Inundation Depth for the next 100 years. Black dots represent the probability of exceedance of tsunami hydrodynamic parameter for each event in the catalog. Blue line is the best fit curve to the data and dashed blue line is the 95% confidence boundary of the fitted curve. Residual of the fit is represented for each probability curve.

Considering the results of the whole simulation, the worst case earthquake scenario generated tsunami waves with maximum water surface elevation equal to 1.8 m, minimum water surface elevation (maximum withdraw) equal to -2.1 m and inundation depth equal to 1.6 m. The probability of occurrence of this event is 35% for next 50 years and 60% for next 100 years.

4.2 Probabilistic Tsunami Inundation Maps for Tuzla Test Site

Inundation maps of Tuzla domain are also prepared for the next 50 and 100-years in GIS environment. Even if inundation depth is in the order of few centimeters, it can lead to dragging of people in coastal regions due to the high current velocities of the waves (Jonkman and Penning-Rowsell, 2008). Therefore, these inundation maps have a great significance to understand the flooded areas in study domain and the amount of water penetrated inland.

Generation of inundation maps are based on the probability of exceedance of 0.3 m inundation depth. There are several studies in literature proving both experimentally and numerically that tsunami waves with the order of 0.3 m height have a potential to collapse a human body (Jonkman and Penning-Rowsell, 2008; Takagi et al., 2016). For this reason, only the earthquake scenarios that generated inundation depths larger than or equal to 0.3 m threshold value are considered.

- Inundation depth files, which is one of the outputs of the NAMI DANCE, are used for the calculation.
- The inundation depth values at each grid node are replaced with the probability of occurrence of the respective earthquake scenario. We repeated this procedure for all earthquake scenarios, which has inundation depths larger than or equal to 0.3 m threshold.

The mean (average) probability of occurrence is calculated at each grid node. Thus, the spatial distribution of probability of

375   exceedance of 0.3 m inundation depth in inundation zone is obtained for a specific time interval (Fig 8).

Figure 8 shows the inundation maps of Tuzla shipyard for the next 50 and 100-years. Most of the area in Tuzla shipyard region have probability of exceedance between 10% and 20% for both of the next 50 and 100 years. However, some places in the northern and southern part of the area and inside the bay show larger than 75% probability of inundation within the next 100 years. Maximum inundation distance is observed as around 60 m in the test site.
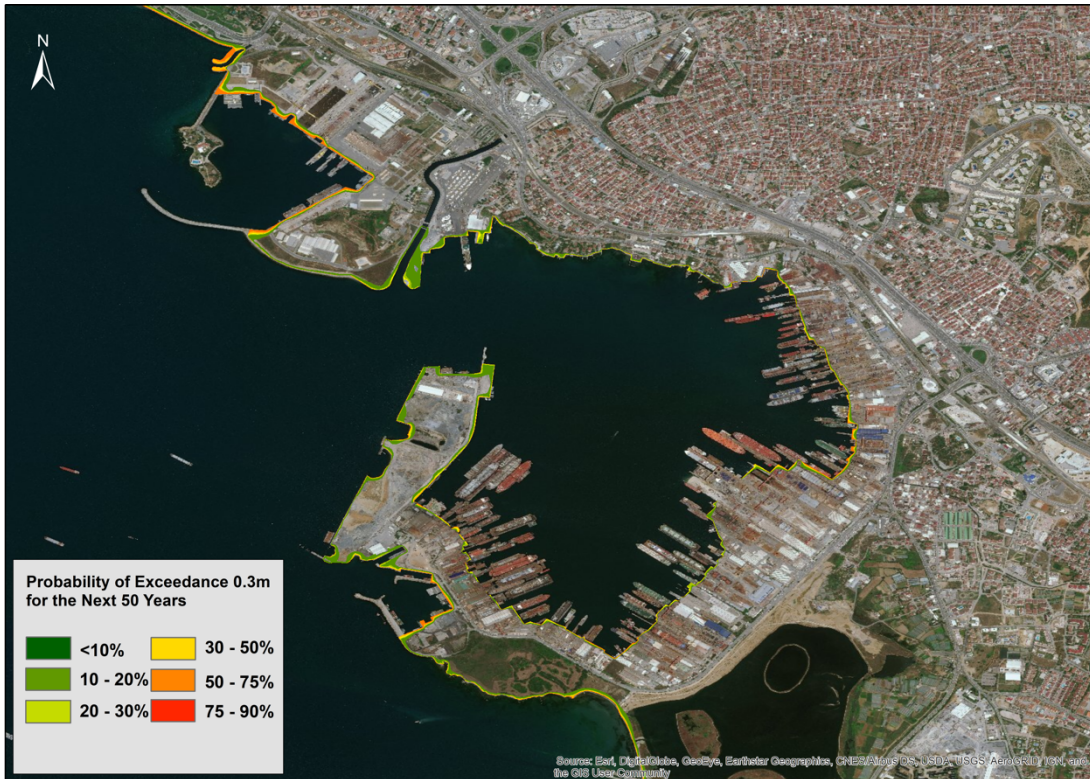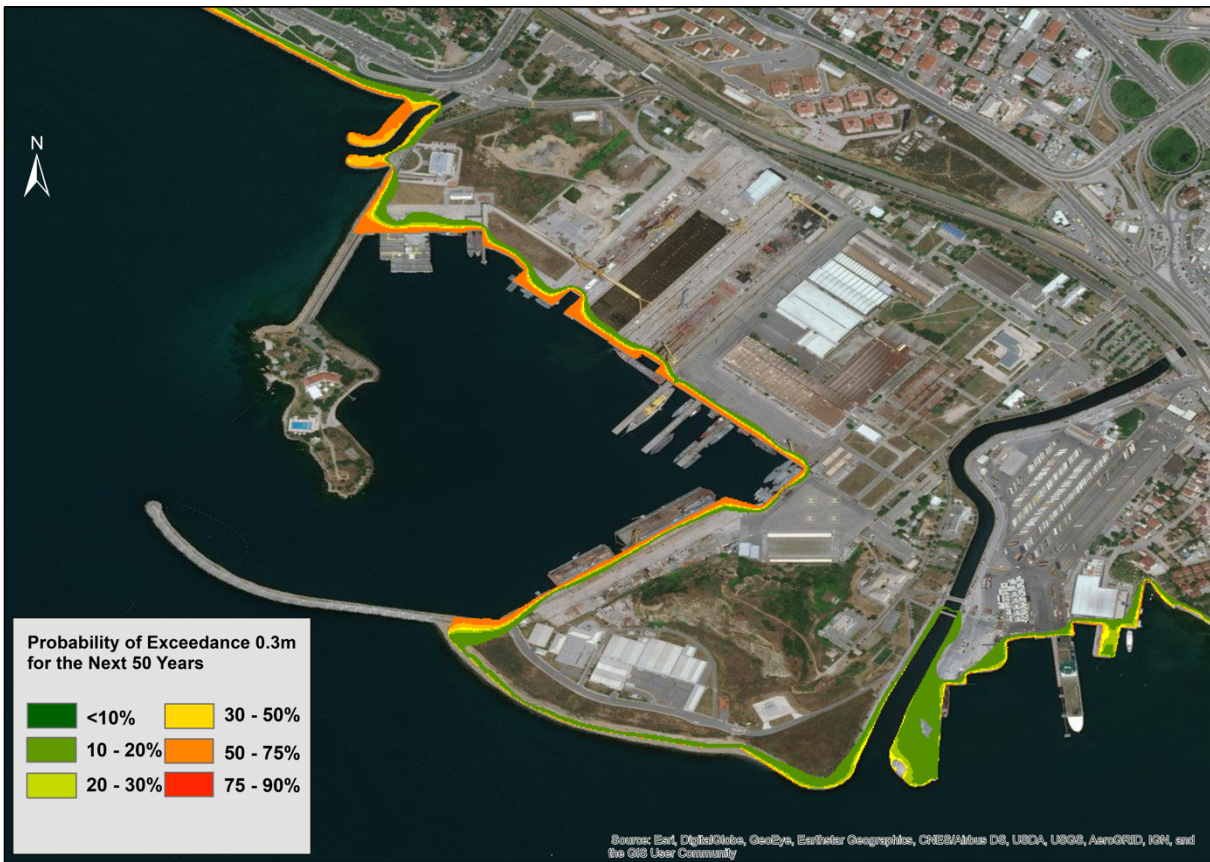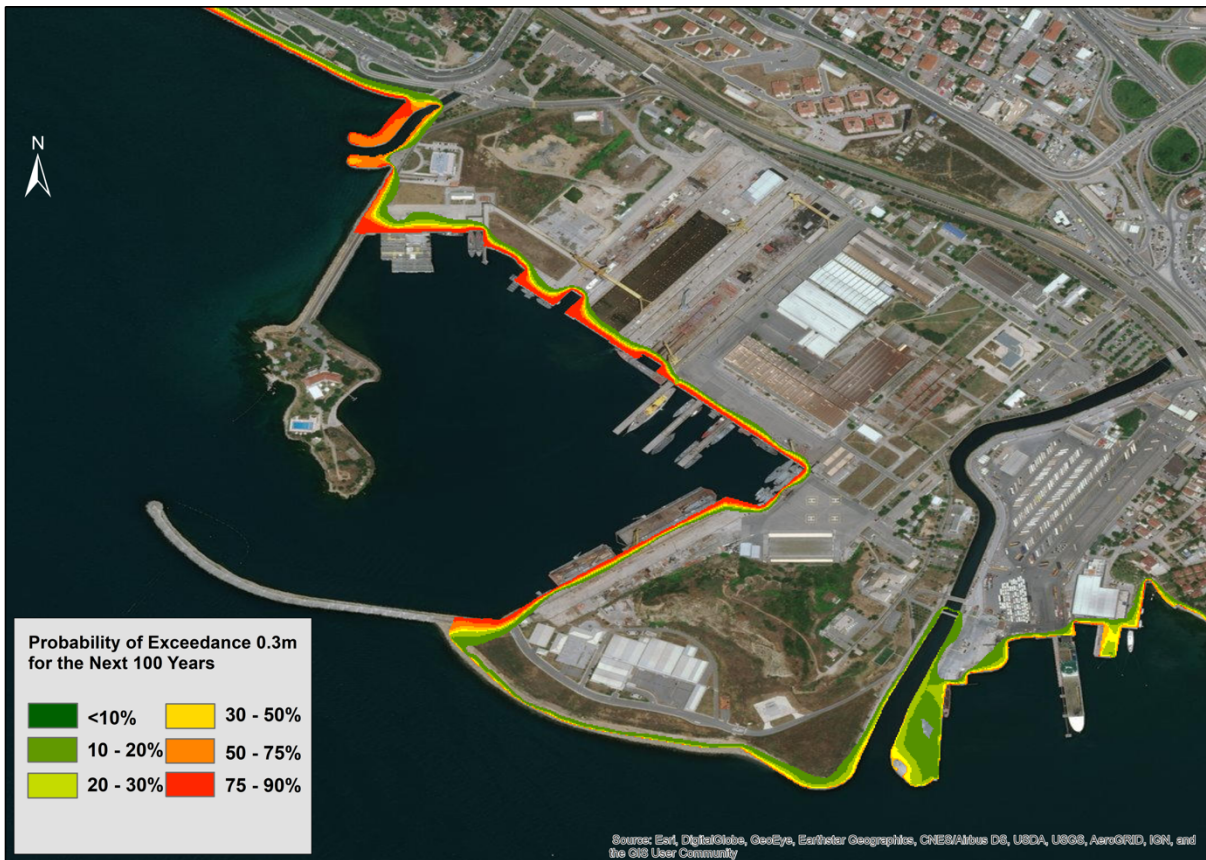

380

Figure 8: Probabilistic Tsunami Inundation Maps for Tuzla Study Domain representing the Probability of Exceedance of 0.3 m Inundation Depth within the Next 50 and 100 Years. Change of colors from green to red represents the increasing probability of exceedance (created using ArcMap Version 10.5).

385   In Figure 9, probabilistic inundation maps of one of the most important facilities in the study region are represented for the next 50 and 100 years. The area has high potential to be exposed to tsunami waves with probability larger than 50% for the next 50 years. In 100 years, this probability increases and varies between 75% and 90%. No significant inundation zone is observed along the coast of the seawall and the peninsula. This may be due to the high ground elevation of these zones. Tsunami waves are inundated up to 45 m inside the small bay. This inundation distance could cause severe damage to shipyard

390   and other constructions if corresponding current velocities are also significant.

Probability of Exceedance 0.3m for the Next 50 Years

<10%	30 - 50%
10 - 20%	50 - 75%
20 - 30%	75 - 90%

Source: Esri, DigitalGlobe, GeoEye, Earthstar Geographics, CNES/Airbus DS, USDA, USGS, AeroGRID, IGN, and the GIS User Community
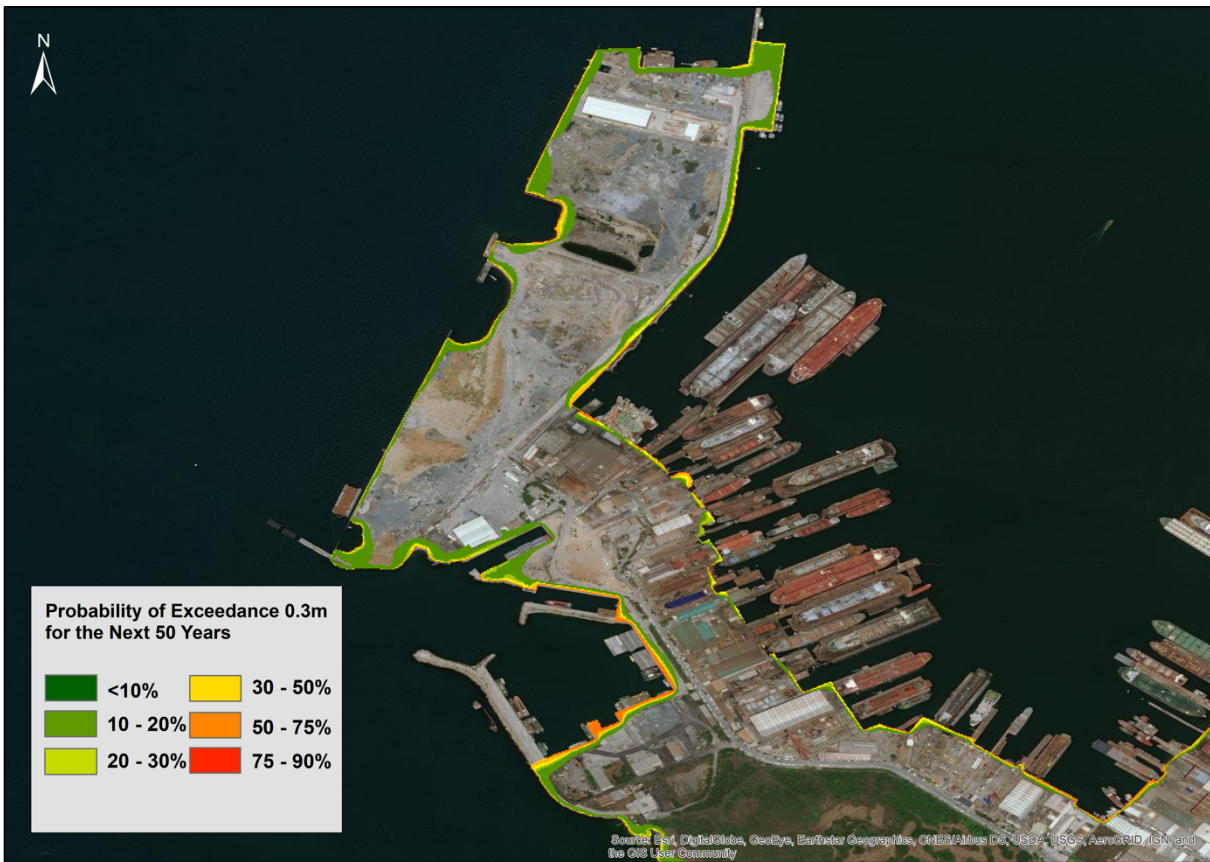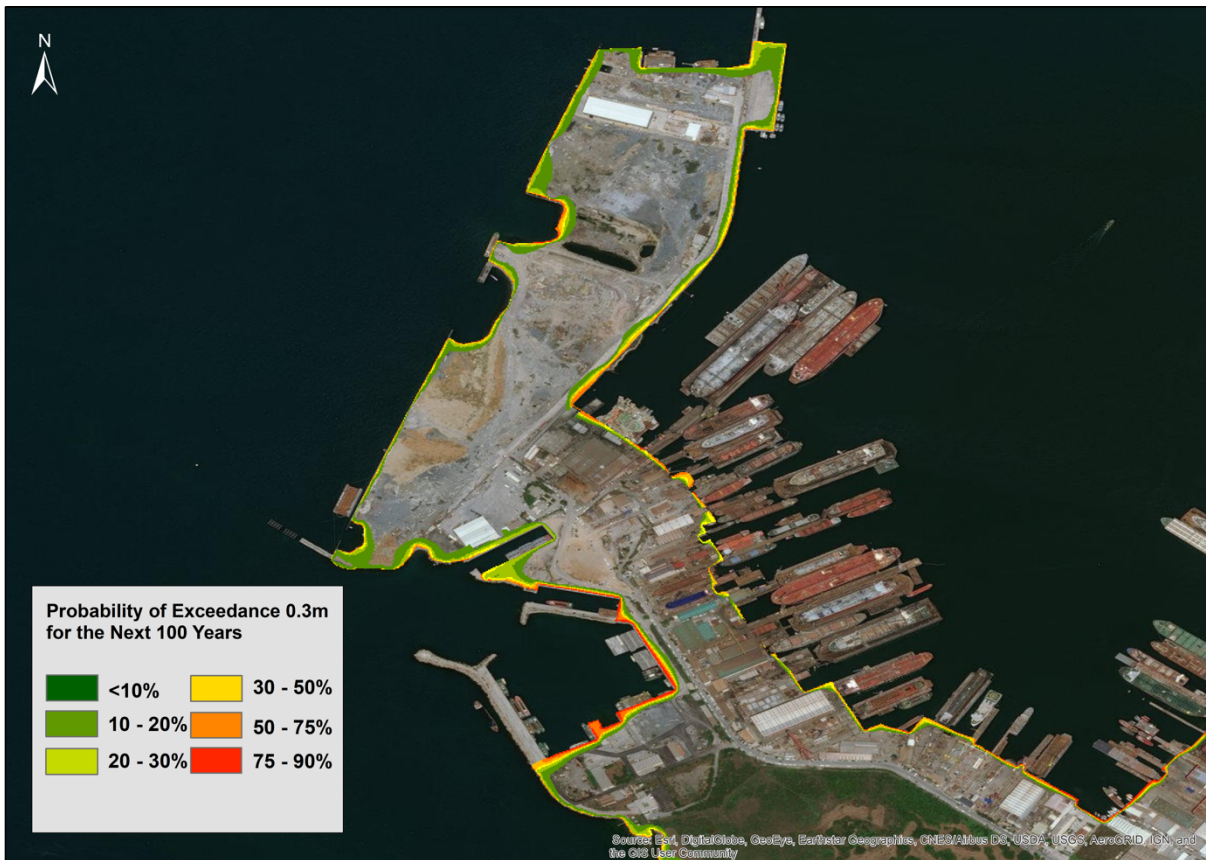
Figure 9: Probabilistic Tsunami Inundation Maps of Northern Part of Tuzla Study Domain representing the Probability of Exceedance of 0.3 m Inundation Depth for the Next 50 and 100 Years. Change of colors from green to red represents the increasing probability of exceedance (created using ArcMap Version 10.5).

In the next figure (10), the southern part of the Tuzla shipyard is seen according to probabilities of inundation for the next 50 and 100 years. Very limited area in the coastal zone is inundated with the probability between 30% and 50% within the next 50 years. The probability reduces up to 10% at some inner locations from the coastline. For 100-year recurrence time, the situation is almost the same. Only minor parts of the region at the south approaches up to 75% - 90% probability of exceedance of 0.3 m inundation depth threshold. The maximum inundation distance is calculated about 60 m. The inundated region does not include any important facility or structure and the effect of the tsunami will be minimal. The inundation distance decreases to 10 m at the other parts of the region.

Probability of Exceedance 0.3m
for the Next 50 Years

<10%		30 - 50%
10 - 20%		50 - 75%
20 - 30%		75 - 90%

Source: Esri, DigitalGlobe, GeoEye, Earthstar Geographics, CNES/Airbus DS, USDA, USGS, AeroGRID, IGN, and the GIS User Community

Figure 10: Probabilistic Tsunami Inundation Maps for the Southern Part of Tuzla Study Domain representing the Probability of Exceedance of 0.3 m Inundation Depth for the Next 50 and 100 Years. Change of colors from green to red represents the increasing probability of exceedance (created using ArcMap Version 10.5).

The region indicated in Fig 11 is located inside the bay and includes a large part of the shipyard area. This area includes lots of large and small piers and ship construction facilities. The situation is more or less the same with the previous region (Fig 9). Probability of having larger than 0.3 m inundation depth changes between 30% and 50% within the next 50 years, while only a few places show 75% - 90% probability for the next 100 years along the coast. Moreover, maximum inundation distance is calculated as 25 m for this zone. Even if the probability of inundation is low, these zones should be taken into consideration before constructing a new structure.

Probability of Exceedance 0.3m for the Next 50 Years

<10%	30 - 50%
10 - 20%	50 - 75%
20 - 30%	75 - 90%

415

Figure 11: Probabilistic Tsunami Inundation Maps of Shipyard Area in Tuzla Study Domain representing the Probability of Exceedance of 0.3 m Inundation Depth for the Next 50 and 100 Years. Change of colors from green to red represents the increasing probability of exceedance (created using ArcMap Version 10.5).
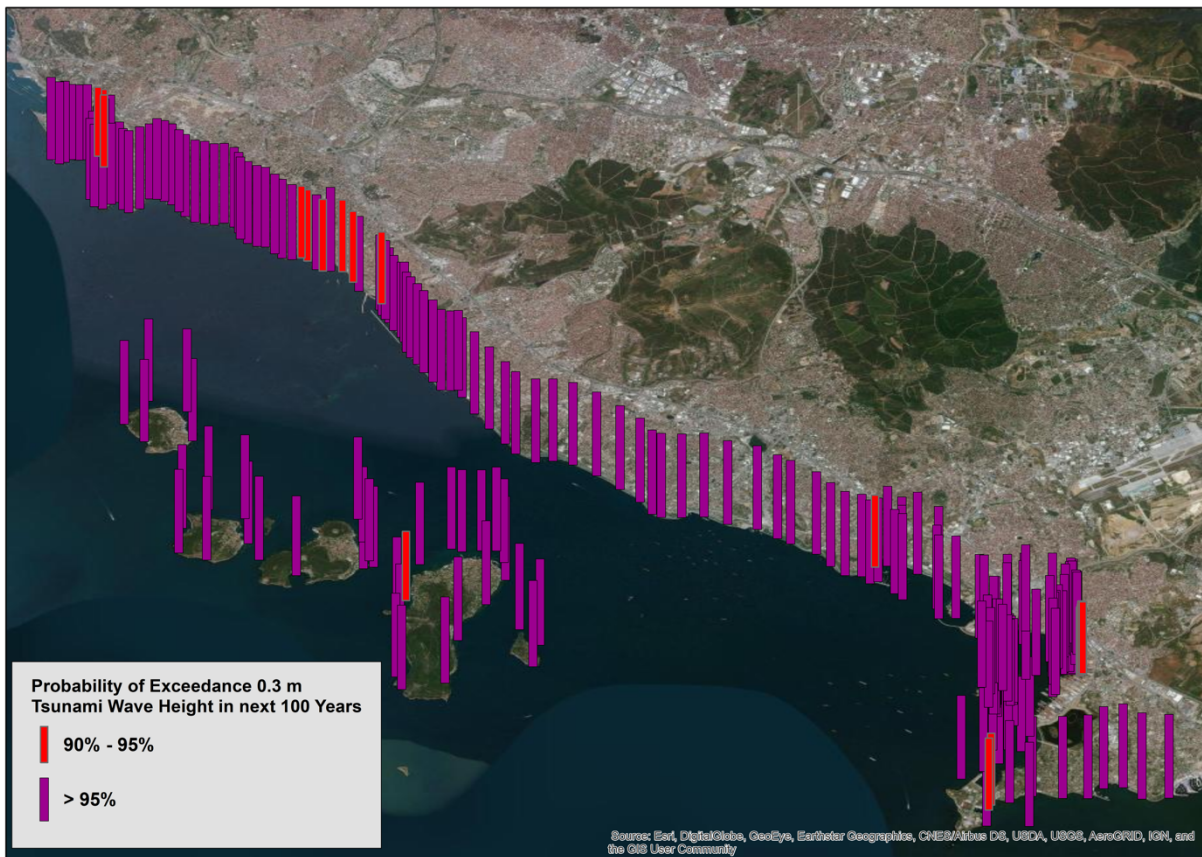
4.3 Synthetic Gauges

Finally, the probability of exceedance of 0.3 m wave heights at synthetic gauge points are presented by bar charts to consider the near shore effect of tsunami waves along the western coast of Istanbul. Because of the closeness to the fault zone, the southeast coasts of the city are under the threat of the significant tsunami damage. Similar with the method applied during the preparation of probabilistic inundation maps, the earthquake scenarios with wave heights at synthetic gauge points larger than or equal to 0.3 m are selected and replaced with the probability of each scenario according to wave heights and after that the average probabilities at each synthetic gauge point are obtained accordingly.

Figure 12 demonstrates the probability of exceedance of 0.3m wave height at synthetic gauge points, which are about 350 m distant from each other, along the western coast of the Istanbul within the next 50 and 100 years. The probability is increasing while color scale chances from green to purple. According to this figure, minimum probability of exceedance is shown as 75% at some points. Except for a few of 228 synthetic gauge points, all points have larger than 90% probability of exceedance of

0.3 m wave height within the next 50-years time scale.

This condition is very serious since there are so many residential areas and important spots such as ports and recreational facilities in this region. The minimum probability of occurrence, which can generate tsunami waves with at least 0.3 m wave heights, reaches up to 90% for the next 100-year time period. However, 95% probability of exceedance of 0.3 m wave height dominates the region for this time scale.
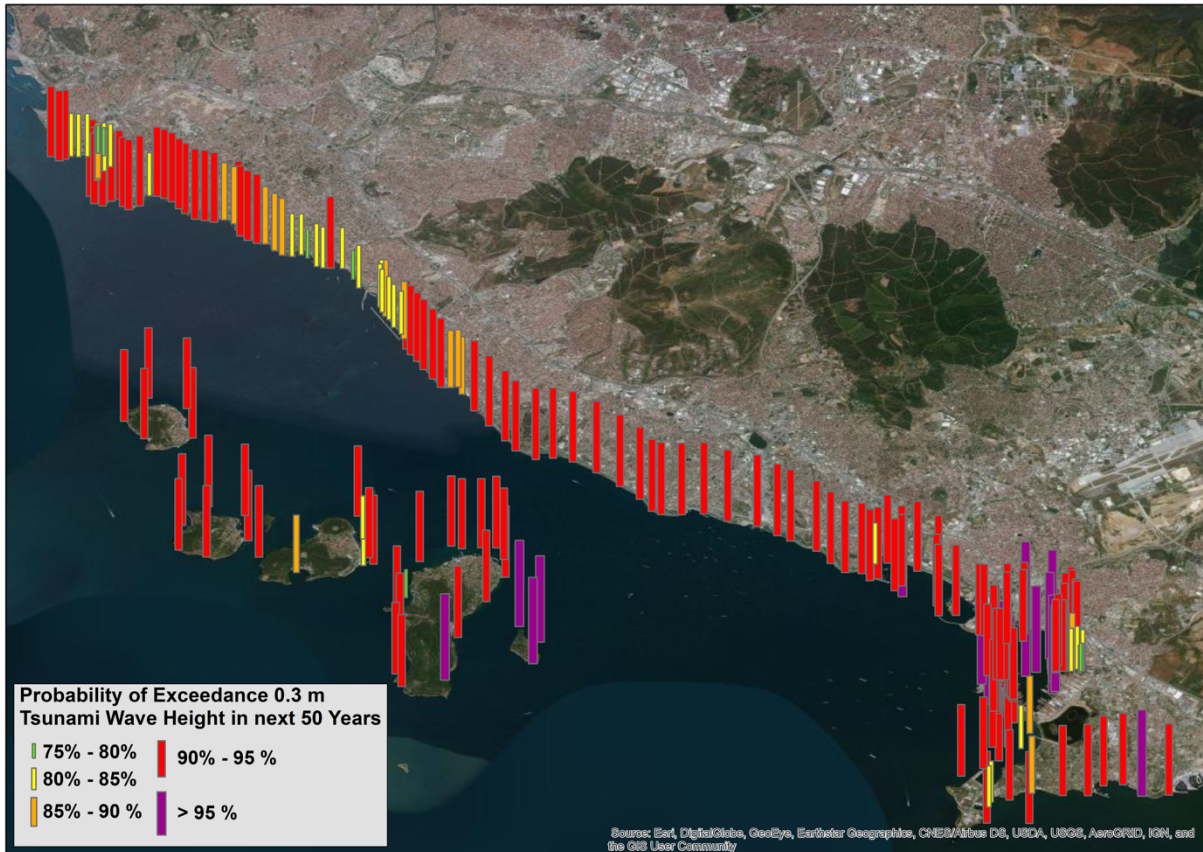
Figure 12: Probability of Exceedance of 0.3 m Tsunami Wave Height within the next 50 and 100 years at Synthetic Gauge Points (yellow rectangles show the Tuzla study domain, change of colors from purple to green on the bars represents the decreasing probability of exceedance (created using ArcMap Version 10.5).

4.4 Uncertainties

PTHA studies include some uncertainties because of the nature of rare occurrence the large events. Quantification of these uncertainties generally includes mixture of empirical analyses and subjective judgment.

Uncertainties of PTHA can be divided into two: as aleatory and epistemic variability. Aleatoric uncertainty is the natural randomness of the physical process. Including more data in the analyses does not contribute to reduce the aleatoric uncertainty. However, knowledge about the modelling process may decrease this unpredictability. The occurrence time of the earthquake is one of the most fundamental aleatory variables in PTHA. This parameter is generally assumed a time-independent variable. However, in this study we used time-dependent probability model which reduces the uncertainty on this parameter. Mechanism of the source is considered as another aleatory variable for PTHA studies. The great number of the earthquakes all round the world occur at well-defined plate boundaries. However, some unidentified low active intraplate faults exist, which are recently contained in PTHA studies (Selva et al., 2016). Moreover, the fault volume, which is used in scaling relations to calculate the

455 source magnitude, is another aleatory term. Although homogenous slip distribution is a common implementation in PTHA, slip distribution of large events do not show homogenous behavior. Therefore, definition of asperities on the fault is another aleatoric variable which should be considered. Tsunami numerical modelling, itself, is also another aleatoric variable since, they do not show correlation with real observations, which are more variable than earthquake scenarios incorporated in PTHA (Grezio et al., 2017). The aleatory variable affects the results because it is incorporated directly into the hazard calculations

460 (Abrahamson and Bommer, 2005).

Epistemic uncertainty, on the other hand, consists of the lack of knowledge of the physical process and data. Segmentation of fault system is one of the epistemic variables since, it is not certain where the rupture will be generated, and which segments will be triggered. In addition, there are many different scaling relations, which cause another epistemic uncertainty, between the fault area and magnitude. It is also important for tsunami generation whether the fault rupture reaches to the surface or not.

465 Thus, updip and downdip limits of the fault rupture can be considered as another epistemic variable (Grezio et al.,2017). Accurate probability distributions of input cannot be known. For example, assuming that probability of occurrence of an event follows Poisson distribution. However, return periods of events do not simply fit to this distribution (Gonzalez et al., 2013). Unlike aleatoric one, epistemic uncertainty can be decreased when more information is available (Godinho, 2007). Different techniques, such as logic tree, Bayesian method etc., have been developed to reduce these uncertainties.

470 In this study, probabilistic model is established based on the characteristic fault model of PIF, which is a segment of NAF one of the best studied fault zones in the world. It is also assumed that the entire fault area is ruptured, reached to the surface and generated a homogenous slip for each event. The maximum magnitude range of the fault is calculated with Wells and Coppersmith (1994) scaling relation. All these assumptions naturally include uncertainties which are naturally reflected to this PTHA study. Besides, MC simulation itself also includes uncertainty as being performed hundred times to create synthetic

475 earthquake scenarios. The effect of uncertainty in aperiodicity parameter is also existing and can be reduced by including different parameters to MC simulation. Therefore, the tsunami hydrodynamic parameters associated with the probability of occurrence of the corresponding scenario preserve the same uncertainty.

5 Conclusion

In this study, time-dependent PTHA is performed in Tuzla region, Istanbul for the purpose of understanding the probability of

480 having tsunami inundation after the PIF rupture. The study combines tsunami numerical modelling with probabilistic approach, which is modified by probabilistic seismic hazard analysis. Probability calculations have been done based on the time-dependent BPT model, which depends on the time period passed since the last characteristic event and the recurrence time of earthquake. After that, synthetic earthquake catalogue is generated using MC simulation technique and tsunami numerical modelling was performed depending on this earthquake catalogue using NAMI DANCE code in GPU environment.

485 Results of this PTHA study was presented in three different ways for the next 50 and 100 years. The first one was the graphs showing the change of probability with the maximum and minimum water surface elevation and inundation depth for different time intervals. Secondly the probabilistic tsunami inundation maps are generated for Tuzla region. Finally, the probability maps of exceedance of 0.3 m wave heights at synthetic gauge points are represented with bar charts.

The main results of this study can be summarized as follows:

490   •   According to the distribution of probability with respect to tsunami hydrodynamic parameters, the probability of exceedance of 1 m maximum positive and negative water surface elevation is 65% within next 50 years. The probability for 1 m inundation depth is 60%.

•   Considering probabilities for next 100 years, 85% probability of exceedance of 1 m was calculated. For 1 m inundation depth, probability of exceedance is obtained about 80%.

495   •   As a result of the whole simulation, 1.8 m, -2.1 m and 1.6 m were calculated for maximum and minimum water surface elevation and inundation depth, respectively with the probability of 35% for the next 50 years, 60% for next 100 years.

•   Inundation maps, indicate that inundation of tsunami waves that are equal to or larger than 0.3 m have probability mostly higher than 10 % and 20% for the next 50 years and 100 years, respectively. The probability of occurrence of

500   0.3m inundation depth was calculated as maximum 75% for the next 100 years. Maximum inundation distance is calculated as 60 m and observed in the southern part of the finest 3m grid-sized study area.

•   Probabilistic results for the exceedance of 0.3 m wave height at synthetic gauge points demonstrate that only few of them have a probability between 75% - 85%, however several points have more than 90% probability for the next 50 years. Probability of exceedance increases by more than 95% for the next 100-years.

505 The tsunami impact of the PIF rupture along the Tuzla coast is very important as proposed with the results of this study. However, as further steps of this study, PTHA can be done for the other critical test sites along the Marmara Sea that are close to the PIF segment. Besides, it is also advantageous to consider the other fault segments, having their various rupture combinations and complex rupture probabilities in Marmara Sea as further studies. Previously in the framework of the MARSite project, tsunami arrival times and maximum wave amplitudes are calculated along the coast of the Marmara Sea

510 using different earthquake scenarios and a tsunami scenario database was obtained in deterministic approach (Ozer Sozdinler et al., 2020). Results of this study show that, arrival time of tsunami waves is very short in Marmara Sea for most of the scenarios which complicates the tsunami early warning operations and evacuation actions. However, due to the short arrival times of first tsunami waves along Marmara coast, the tsunami inundation scenario databases would be of great importance in such conditions. It would be the best option for the decision makers and civil protection authorities to have the inundation

515 maps prepared also in probabilistic approach in order to realize the possibility of exceedance of selected threshold inundation depth for certain critical coastal locations.

This study shows a methodology for PTHA with time – dependent probabilistic model using only one fault (PIF) as earthquake and tsunami source. Furthermore, this study can be developed including some connected faults to the PIF in both time – dependent and time - independent probability calculations and BPT probability can be combined with static Coulomb stress

520 changes on the faults. BPT model can also be improved by including different aperiodicity parameters. The probability of occurrence of earthquakes is the main focus of this study to perform tsunami hazard analyses. However, submarine landslides are other critical important sources for tsunami generation in Marmara Sea. Probabilities of sliding areas and the sliding

volumes can be considered in the analyses. Submarine landslide generated tsunamis can be coupled with the earthquake triggered tsunamis in order to obtain integrated PTHA in the Marmara Sea.

Acknowledgements

References

Abrahamson, N. A., and Bommer, J. J.: Probability and uncertainty in seismic hazard analysis, Earthquake spectra 21(2), 603-607, https://doi.org/10.1193/1.1899158, 2005.

Aki, K.: Generation and propagation of G waves from the Niigata Earthquake of June 16 1964. Part 2. Estimation of earthquake movement, released energy, and stress-strain drop from the G wave spectrum, Bull. Earthq. Res. Inst., 44, 73-88, https://ci.nii.ac.jp/naid/10006221613/en/, 1966.

Aki, K.: Asperities, barriers, characteristic earthquakes and strong motion prediction, Journal of Geophysical Research: Solid Earth, 89(B7), 5867-5872, **https://doi.org/10.1029/JB089iB07p05867**, 1984.

Aksu, A. E., Calon, T. J., Hiscott, R. N., and Yasar, D.:Anatomy of the North Anatolian Fault Zone in the Marmara Sea, Western Turkey: extensional basins above a continental transform, Gsa Today 10(6), 3-7, 2000.

Allen, C. R: The tectonic environments of seismically active and inactive areas along the San Andreas fault system, Stanford University Publications, Geological Sciences, 11, 70-80, 1968.

Alpar, B., and Yaltırak, C.: Characteristic features of the North Anatolian Fault in the eastern Marmara region and its tectonic evolution. Marine Geology, 190(1-2), 329-350, https://doi.org/10.1016/S0025-3227(02)00353-5, 2002.

Altınok, Y., Alpar, B., and Yaltırak, C.: Şarköy-Mürefte 1912 earthquake's tsunami, extension of the associated faulting in the Marmara Sea, Turkey, Journal of Seismology, 7(3), 329-346, https://doi.org/10.1023/A:1024581022222, 2003.

Altınok, Y. and Alpar, B.: Marmara Island earthquakes, of 1265 and 1935; Turkey, Nat. Hazards Earth Syst. Sci., 6, 999–1006, https://doi.org/10.5194/nhess-6-999-2006, 2006.

Altinok, Y., Alpar, B., Özer, N., and Aykurt, H.: Revision of the tsunami catalogue affecting Turkish coasts and surrounding regions, Nat. Hazards Earth Syst. Sci., 11, 273-291, https://doi.org/10.5194/nhess-11-273-2011, 2011.

Ambraseys, N. N. N., and Finkel, C. F.: Seismicity of Turkey and Adjacent Areas: A Historical Review 1500-1800, MS Eren, 1995.

Ambraseys, N. N., and Jackson, J. A.: Seismicity of the Sea of Marmara (Turkey) since 1500, Geophysical Journal International 141(3), F1-F6, https://doi.org/10.1046/j.1365-246x.2000.00137.x, 2000.

Ambraseys, N.: The seismic activity of the Marmara Sea region over the last 2000 years, Bulletin of the Seismological Society of America, 92(1) 1-18, https://doi.org/10.1785/0120000843, 2002.

Annaka, T., Satake, K., Sakakiyama, T., Yanagisawa, K., & Shuto, N.: Logic-tree approach for probabilistic tsunami hazard analysis and its applications to the Japanese coasts, In Tsunami and its hazards in the indian and pacific oceans (pp. 577-592). Birkhäuser Basel, https://doi.org/10.1007/978-3-7643-8364-0_17, 2007.

Armijo, R., Meyer, B., Hubert, A., and Barka, A.: Westward propagation of the North Anatolian fault into the northern Aegean: Timing and kinematics, Geology 27(3) 267-270, https://doi.org/10.1130/0091-7613(1999)027<0267:WPOTNA>2.3.CO;2, 1999.

Armijo, R., Meyer, B., Navarro, S., King, G., and Barka, A.: Asymmetric slip partitioning in the Sea of Marmara pull-apart: A clue to propagation processes of the North Anatolian fault?, Terra Nova 14(2), 80-86, https://doi.org/10.1046/j.1365-3121.2002.00397.x, 2002.

Armijo, R., Pondard, N., Meyer, B., Uçarkus, G., de Lépinay, B. M., Malavieille, J., ... and Cagatay, N.: Submarine fault scarps in the Sea of Marmara pull-apart (North Anatolian Fault): Implications for seismic hazard in Istanbul, Geochemistry, Geophysics, Geosystems, 6(6), https://doi.org/10.1029/2004GC000896, 2005.

Aytore, B., Yalciner, A. C., Zaytsev, A., Cankaya, Z. C., and Suzen, M. L.: Assessment of tsunami resilience of Haydarpaşa Port in the Sea of Marmara by high-resolution numerical modeling, Earth, Planets and Space, 68(1), 139, https://doi.org/10.1186/s40623-016-0508-z, 2016.

Bohnhoff, M., Bulut, F., Dresen, G., Malin, P. E., Eken, T., and Aktar, M.: An earthquake gap south of Istanbul, Nature communications, 4 1999, https://doi.org/10.1038/ncomms2999, 2013.

Barka, A.: The 17 august 1999 Izmit earthquake, Science 285(5435) 1858-1859, https://doi.org/10.1126/science.285.5435.1858 , 1999.

Cankaya, Z. C., Suzen, M. L., Yalciner, A. C., Kolat, C., Zaytsev, A., and Aytore, B.: A new GIS-based tsunami risk evaluation: MeTHuVA (METU tsunami human vulnerability assessment) at Yenikapı, Istanbul, Earth, Planets and Space, 68(1), 133, https://doi.org/10.1186/s40623-016-0507-0, 2016.

Cramer, C. H., Petersen, M. D., Cao, T., Toppozada, T. R., and Reichle, M.: A time-dependent probabilistic seismic-hazard model for California, Bulletin of the Seismological Society of America, 90(1), 1-21, https://doi.org/10.1785/0119980087, 2000.

Davis, P. M., Jackson, D. D., and Kagan, Y. Y.: The longer it has been since the last earthquake, the longer the expected time till the next?, Bulletin of the Seismological Society of America, 79(5), 1439-1456, 1989.

Earthquake Research Committee: Evaluation method and its application for the probability of long-term earthquke occurrence (in Japanese). Headquarters for Earthquake Research Promotion, Tokyo, 2001.

Ellsworth, W. L., Matthews, M. V., Nadeau, R. M., Nishenko, S. P., Reasenberg, P. A., and Simpson, R. W.: A physically-based earthquake recurrence model for estimation of long-term earthquake probabilities, US Geol. Surv. Open-File Rept. 99, 522, 23, 1999.

Emre, Ö., Duman, T. Y., Özalp, S., Elmacı, H., Olgun, Ş., and Şaroğlu, F.: Active fault map of Turkey with explanatory text, General Directorate of Mineral Research and Exploration Special Publication Series, 30, 2013.

Ergintav, S., Reilinger, R. E., Çakmak, R., Floyd, M., Cakir, Z., Doğan, U., and Özener, H.: Istanbul's earthquake hot spots: Geodetic constraints on strain accumulation along faults in the Marmara seismic gap, Geophysical Research Letters, 41(16), 5783-5788, https://doi.org/10.1002/2014GL060985, 2014.

Erdik, M., Demircioglu, M., Sesetyan, K., Durukal, E., and Siyahi, B.: Earthquake hazard in Marmara region, Turkey, Soil Dynamics and Earthquake Engineering 24(8), 605-631, https://doi.org/10.1016/j.soildyn.2004.04.003, 2004.

Flerit, F., Armijo, R., King, G. C. P., Meyer, B., and Barka, A.: Slip partitioning in the Sea of Marmara pull-apart determined from GPS velocity vectors, Geophysical Journal International 154(1) 1-7, https://doi.org/10.1046/j.1365-246X.2003.01899.x, 2003.

Flerit, F., Armijo, R., King, G., and Meyer, B.: The mechanical interaction between the propagating North Anatolian Fault and the back-arc extension in the Aegean, Earth and Planetary Science Letters 224(3-4), 347-362, https://doi.org/10.1016/j.epsl.2004.05.028, 2004.

Gasperini, L., Polonia, A., Çağatay, M. N., Bortoluzzi, G., and Ferrante, V.: Geological slip rates along the North Anatolian Fault in the Marmara region, Tectonics, 30(6), **https://doi.org/10.1029/2011TC002906**, 2011.

610 Geist, E. L., and Parsons, T.: Probabilistic analysis of tsunami hazards, Natural Hazards, 37(3) 277-314, https://doi.org/10.1007/s11069-005-4646-z, 2006.

Geist, E.L., and P.J. Lynett.:Source processes for the probabilistic assessment of tsunami hazards. Oceanography 27(2):86–93, http://dx.doi.org/10.5670/oceanog.2014.43, 2014.

Goda, K., and De Risi, R.: Multi-hazard loss estimation for shaking and tsunami using stochastic rupture

615 sources, International journal of disaster risk reduction, 28, 539-554, https://doi.org/10.1016/j.ijdrr.2018.01.002, 2018.

Godinho, J.: Probabilistic Seismic Hazard Analysis an Introduction to Theoretical Basis and Applied Methodology, Mcs. thesis, University of Patras, Greece, 2007.

González, F. I., Geist, E. L., Jaffe, B., Kânoğlu, U., Mofjeld, H., Synolakis, C. E., ... and Horning, T.: Probabilistic tsunami hazard assessment at seaside, Oregon, for near-and far-field seismic sources, Journal of Geophysical Research: Oceans

620 114(C11), https://doi.org/10.1029/2008JC005132, 2009.

Gonzalez, F. I., LeVeque, R. J., and Adams, L. M.: Probabilistic Tsunami Hazard Assessment (PTHA) for Crescent City, CA. Final Report for Phase I. University of Washington Department of Applied Mathmatics, http://hdl.handle.net/1773/25916, 2013.

Grezio, A., Babeyko, A., Baptista, M. A., Behrens, J., Costa, A., Davies, G., ... and Harbitz, C. B. : Probabilistic tsunami

625 hazard analysis: Multiple sources and global applications, Reviews of Geophysics, 55(4) 1158-1198, https://doi.org/10.1002/2017RG000579, 2017.

Gutenberg, B., and Richter, C. F.: Frequency of earthquakes in California, Bulletin of the Seismological society of America, 34(4), 185-188, 1944.

Guler, H. G., Arikawa, T., Oei, T., and Yalciner, A. C.: Performance of rubble mound breakwaters under tsunami attack, a

630 case study: Haydarpasa Port, Istanbul, Turkey, Coastal Engineering, 104, 43-53, https://doi.org/10.1016/j.coastaleng.2015.07.007, 2015.

Hancilar, U.: Identification of elements at risk for a credible tsunami event for Istanbul, Nat. Hazards Earth Syst. Sci., 12, 107-119, https://doi.org/10.5194/nhess-12-107-2012, 2012.

Hébert, H., Schindele, F., Altinok, Y., Alpar, B., and Gazioglu, C.:Tsunami hazard in the Marmara Sea (Turkey): a

635 numerical approach to discuss active faulting and impact on the Istanbul coastal areas. Marine Geology, 215(1-2), 23-43, https://doi.org/10.1016/j.margeo.2004.11.006 ,2005.

Hergert, T., and Heidbach, O.: Slip-rate variability and distributed deformation in the Marmara Sea fault system, Nature Geoscience, 3(2) 132, https://doi.org/10.1038/ngeo739, 2010.

Hergert, T., Heidbach, O., Bécel, A., and Laigle, M.: Geomechanical model of the Marmara Sea region—I. 3-D

640 contemporary kinematics, Geophysical Journal International, 185(3), 1073-1089, https://doi.org/10.1111/j.1365-246X.2011.04991.x, 2011.

Horspool, N., Pranantyo, I., Griffin, J., Latief, H., Natawidjaja, D. H., Kongko, W., Cipta, A., Bustaman, B., Anugrah, S. D., and Thio, H. K.: A probabilistic tsunami hazard assessment for Indonesia, Nat. Hazards Earth Syst. Sci., 14, 3105–3122, https://doi.org/10.5194/nhess-14-3105-2014, 2014.

645 Imamura, F.: Tsunami Numerical Simulation with the Staggered Leap-frog Scheme (Numerical code of TUNAMI-N1), School of Civil Engineering, Asian Institute Technical and Disaster Control Research Center, Tohoku University, Tohoku, 1989.

Imamura, F., A.C. Yalçıner, A. C. and G. Özyurt, TUNAMI-N2: Tsunami Modelling Manual, 2001.

Imren, C., Le Pichon, X., Rangin, C., Demirbağ, E., Ecevitoğlu, B., and Görür, N.: The North Anatolian Fault within the Sea

650 of Marmara: a new interpretation based on multi-channel seismic and multi-beam bathymetry data, Earth and Planetary Science Letters 186(2) 143-158, https://doi.org/10.1016/S0012-821X(01)00241-2, 2001.

Insel, I., The Effects of the Material Density and Dimensions of the Landslide on the Generated Tsunamis, Mcs.Thesis, Middle East Technical University, Ankara,Turkey, 2009.

Jonkman, S. N., and Penning-Rowsell, E.: Human instability in Flood Flows, JAWRA Journal of the American Water

655 Resources Association, 44.5, 1208-1218, https://doi.org/10.1111/j.1752-1688.2008.00217.x, 2008.

Kaneko, F.: A simulation analysis of possible tsunami affecting the Istanbul coast, Turkey, In International Workshop on Tsunami Hazard Assessment and Management in Bangladesh, 2009.

Karabulut, H., Bouin, M. P., Bouchon, M., Dietrich, M., Cornou, C., and Aktar, M.: The seismicity in the eastern Marmara Sea after the 17 August 1999 Izmit earthquake, Bulletin of the Seismological Society of America, 92(1), 387-393, http://dx.doi.org/10.1785/0120000820, 2002.

Karabulut, H., Özalaybey, S., Taymaz, T., Aktar, M., Selvi, O., and Kocaoğlu, A.: A tomographic image of the shallow crustal structure in the Eastern Marmara, Geophysical research letters, 30(24), https://doi.org/10.1029/2003GL018074, 2003.

Kanamori, H.: The diversity of the physics of earthquakes, Proceedings of the Japan Academy, Series B, 80(7) 297-316, https://doi.org/10.2183/pjab.80.297, 2004.

Latcharote, P., Suppasri, A., Imamura, F., Aytore, B., and Yalciner, A. C.: Possible worst-case tsunami scenarios around the Marmara Sea from combined earthquake and landslide sources. In Global Tsunami Science: Past and Future, Volume I (pp. 3823-3846). Birkhäuser, Cham, https://doi.org/10.1007/s00024-016-1411-z, 2016.

Le Pichon, X., Şengör, A. M. C., Demirbağ, E., Rangin, C., Imren, C., Armijo, R., ..and Saatçılar, R.: The active main Marmara fault, Earth and Planetary Science Letters 192(4), 595-616, https://doi.org/10.1016/S0012-821X(01)00449-6, 2001.

Le Pichon, X., Chamot-Rooke, N., Rangin, C., and Sengör, A. M. C.: The North Anatolian fault in the sea of Marmara, Journal of Geophysical Research Solid Earth 108(B4), https://doi.org/10.1029/2002JB001862, 2003.

Le Pichon, X., Imren, C., Rangin, C., Şengör, A. C., and Siyako, M.: The South Marmara Fault, International Journal of Earth Sciences, 103(1), 219-231, https://doi.org/10.1007/s00531-013-0950-0, 2014.

Le Pichon, X., Şengör, A. C., Kende, J., İmren, C., Henry, P., Grall, C., and Karabulut, H.: Propagation of a strike-slip plate boundary within an extensional environment: the westward propagation of the North Anatolian Fault, Canadian Journal of Earth Sciences, 53(11) 1416-1439, https://doi.org/10.1139/cjes-2015-0129, 2015.

Lorito, S., Selva, J., Basili, R., Romano, F., Tiberti, M. M., and Piatanesi, A.: Probabilistic hazard for seismically induced tsunamis: accuracy and feasibility of inundation maps, Geophysical Journal International, 200(1), 574-588, https://doi.org/10.1093/gji/ggu408, 2015.

Løvholt, F., Glimsdal, S., Harbitz, C. B., Zamora, N., Nadim, F., Peduzzi, P., and Smebye, H.: Tsunami hazard and exposure on the global scale, Earth-Science Reviews, 110(1-4), 58-73, https://doi.org/10.1016/j.earscirev.2011.10.002, 2012.

Løvholt, F., Griffin, J., and Salgado-Gálvez, M.: Tsunami hazard and risk assessment at a global scale, Encyclopedia of complexity and systems science, 1-34, https://doi.org/10.1007/978-3-642-27737-5_642-1, 2015

Lynett, P. J., Gately, K., Wilson, R., Montoya, L., Arcas, D., Aytore, B., and David, C. G.: Inter-model analysis of tsunami-induced coastal currents, Ocean Modelling 114 14-32, https://doi.org/10.1016/j.ocemod.2017.04.003, 2017.

Matthews, M. V., Ellsworth, W. L., and Reasenberg, P. A.: A Brownian model for recurrent earthquakes, Bulletin of the Seismological Society of America, 92(6), 2233-2250, https://doi.org/10.1785/0120010267, 2002.

Meade, B. J., Hager, B. H., McClusky, S. C., Reilinger, R. E., Ergintav, S., Lenk, O., … and Ozener, H.: Estimates of seismic potential in the Marmara Sea region from block models of secular deformation constrained by Global Positioning System measurements, Bulletin of the Seismological Society of America, 92(1) 208-215, https://doi.org/10.1785/0120000837, 2002.

McNeill, L. C., Mille, A., Minshull, T. A., Bull, J. M., Kenyon, N. H., and Ivanov, M.: Extension of the North Anatolian Fault into the North Aegean Trough: Evidence for transtension, strain partitioning, and analogues for Sea of Marmara basin models, Tectonics 23(2), https://doi.org/10.1029/2002TC001490, 2004.

Murru, M., Akinci, A., Falcone, G., Pucci, S., Console, R., and Parsons, T.: M≥ 7 earthquake rupture forecast and time-dependent probability for the Sea of Marmara region Turkey, Journal of Geophysical Research: Solid Earth 121(4) 2679-2707, https://doi.org/10.1002/2015JB012595, 2016.

NAMI DANCE: Manual of Numerical Code NAMI DANCE, published in http://namidance.ce.metu.edu.tr, 2011.

NTHMP, Proceedings and Results of the National Tsunami Hazard Mitigation Program 2015 Tsunami Current Modeling Workshop, Portland, Oregon, 2015.

Oglesby, D. D., and Mai, P. M.: Fault geometry, rupture dynamics and ground motion from potential earthquakes on the North Anatolian Fault under the Sea of Marmara, Geophysical Journal International, 188(3), 1071-1087, https://doi.org/10.1111/j.1365-246X.2011.05289.x, 2012.

Okada, Y.: Surface deformation due to shear and tensile faults in a half-space, Bulletin of the seismological society of America, 75(4) 1135-1154, 1985.

Okay, A. I., Demirbağ, E., Kurt, H., Okay, N., and Kuşçu, İ.: An active, deep marine strike-slip basin along the North Anatolian fault in Turkey,Tectonics 18(1) 129-147, https://doi.org/10.1029/1998TC900017, 1999.

Ozer Sozdinler, C., O. Necmioglu, Bayraktar H. B. and Ozel N.M.: Tectonic Origin Tsunami Scenario Database for the Marmara Region, Nat. Hazards Earth Syst. Sci., Manuscript submitted for publication, in peer review, 2020.

710 Parsons, T.: Recalculated probability of M≥ 7 earthquakes beneath the Sea of Marmara, Turkey, Journal of Geophysical Research:Solid Earth 109(B5), https://doi.org/10.1029/2003JB002667, 2004.

Petersen, M. D., Cao, T., Campbell, K. W., and Frankel, A. D.: Time-independent and time-dependent seismic hazard assessment for the State of California: Uniform California Earthquake Rupture Forecast Model 1.0, Seismological Research Letters, 78(1), 99-109, https://doi.org/10.1785/gssrl.78.1.99, 2007.

715 Pondard, N., Armijo, R., King, G. C., Meyer, B., and Flerit, F.: Fault interactions in the Sea of Marmara pull-apart (North Anatolian Fault): earthquake clustering and propagating earthquake sequences, Geophysical Journal International 171(3) 1185-1197, https://doi.org/10.1111/j.1365-246X.2007.03580.x, 2007.

Reilinger, R., McClusky, S., Vernant, P., Lawrence, S., Ergintav, S., Cakmak, R., ... and Nadariya, M.: GPS constraints on continental deformation in the Africa-Arabia-Eurasia continental collision zone and implications for the dynamics of plate

720 interactions, Journal of Geophysical Research: Solid Earth 111(B5), https://doi.org/10.1029/2005JB004051, 2006.

Ren, J., and Zhang, S.: Estimation of recurrence interval of large earthquakes on the Central Longmen Shan fault zone based on seismic moment accumulation/release model, The Scientific World Journal, http://dx.doi.org/10.1155/2013/458341, 2013.

Rikitake, T.: Probability of earthquake occurrence as estimated from crustal strain, Tectonophysics, 23(3), 299-312, https://doi.org/10.1016/0040-1951(74)90029-8, 1974.

725 Ryall, A., Slemmons, D. B., and Gedney, L. D.: Seismicity, tectonism, and surface faulting in the western United States during historic time, Bulletin of the Seismological Society of America, 56(5), 1105-1135, 1966.

Schwartz, D. P., and Coppersmith, K. J.: Fault behavior and characteristic earthquakes: Examples from the Wasatch and San Andreas fault zones, Journal of Geophysical Research: Solid Earth, 89(B7), 5681-5698, **https://doi.org/10.1029/JB089iB07p05681**, 1984.

730 Selva, J., Tonini, R., Molinari, I., Tiberti, M. M., Romano, F., Grezio, A., and Lorito, S.: Quantification of source uncertainties in seismic probabilistic tsunami hazard analysis (SPTHA), Geophysical Journal International, 205(3), 1780-1803, https://doi.org/10.1093/gji/ggw107, 2016.

Shuto, N., Goto, C., and Imamura, F.:Numerical simulation as a means of warning for near-field tsunamis, Coastal Engineering in Japan, 33(2) 173-193, https://doi.org/10.1080/05785634.1990.11924532, 1990.

735 Sørensen, M. B., Spada, M., Babeyko, A., Wiemer, S., and Grünthal, G.:Probabilistic tsunami hazard in the Mediterranean Sea, Journal of Geophysical Research: Solid Earth 117(B1), https://doi.org/10.1029/2010JB008169, 2012.

Stein, R. S., Barka, A. A., and Dieterich, J. H.: Progressive failure on the North Anatolian fault since 1939 by earthquake stress triggering, Geophysical Journal International 128(3), 594-604, https://doi.org/10.1111/j.1365-246X.1997.tb05321.x, 1997.

740 Synolakis, C. E., Bernard, E. N., Titov, V. V., Kânoğlu, U., and González, F. I.: Standards, Criteria, and Procedures for NOAA Evaluation of Tsunami Numerical Models, 2007.

Synolakis, C. E., Bernard, E. N., Titov, V. V., Kânoğlu, U., and Gonzalez, F. I.: Validation and verification of tsunami numerical models. In Tsunami Science Four Years after the 2004 Indian Ocean Tsunami, pp. 2197-2228, Birkhäuser, Basel, 2008.

745 Şengör, A. C., Grall, C., İmren, C., Le Pichon, X., Görür, N., Henry, P., and Siyako, M.: The geometry of the North Anatolian transform fault in the Sea of Marmara and its temporal evolution: implications for the development of intracontinental transform faults, Canadian Journal of Earth Sciences, 51(3), 222-242, https://doi.org/10.1139/cjes-2013-0160, 2014.

Takagi, H., Mikami, T., Fujii, D., Esteban, M., and Kurobe, S.: Mangrove forest against dyke-break-induced tsunami on rapidly subsiding coasts, Nat. Hazards Earth Syst. Sci., 16, 1629-1638, https://doi.org/10.5194/nhess-16-1629-2016, 2016.

750 Tinti, S., Armigliato, A., Manucci, A., Pagnoni, G., Zaniboni, F., Yalçiner, A. C., and Altinok, Y. (2006): The generating mechanisms of the August 17, 1999 Izmit bay (Turkey) tsunami: regional (tectonic) and local (mass instabilities) causes, Marine Geology, 225(1-4), 311-330, https://doi.org/10.1016/j.margeo.2005.09.010, 2006.

Tufekci, D., Suzen, M. L., Yalciner, A. C., and Zaytsev, A.: Revised MeTHuVA method for assessment of tsunami human vulnerability of Bakirkoy district, Istanbul. Natural hazards, 90(2), 943-974, https://doi.org/10.1007/s11069-017-3082-1,

755 2018.

Utkucu, M., Kanbur, Z., Alptekin, Ö., and Sünbül, F.: Seismic behaviour of the North Anatolian Fault beneath the Sea of Marmara (NW Turkey): implications for earthquake recurrence times and future seismic hazard, Natural hazards, 50(1), 45-71, https://doi.org/10.1007/s11069-008-9317-4, 2009.

760 Velioglu, D., Advanced Two and Three Dimensional Tsunami Models: Benchmarking and Validation, Msc. Thesis, Middle East Technical University, Ankara, Tukey, 2009.

Wells, D. L., and Coppersmith, K. J.: New empirical relationships among magnitude, rupture length, rupture width, rupture area, and surface displacement., Bulletin of the seismological Society of America, 84(4), 974-1002, 1994.

Wessel, P., and Smith, W. H.: New, improved version of Generic Mapping Tools released, Eos, Transactions American Geophysical Union, 79(47), 579-579, https://doi.org/10.1029/98EO00426, 1998.

765 Working Group on California Earthquake Probabilities: Earthquake probabilities in the San Francisco Bay Region: 2000 to 2030 a summary of findings, U.S. Geol. Surv. Open-File Rept. 99–517, 1999.

WGCEP (Working Group on California Earthquake Probabilities): Earthquake probabilities in the San Francisco Bay region: 2002–2031, US Geological Survey Open-File Report 03-214, 2003.

Wong, H. K., Lüdmann, T., Ulug, A., and Görür, N.: The Sea of Marmara: a plate boundary sea in an escape tectonic 770 regime, Tectonophysics 244(4) 231-250, https://doi.org/10.1016/0040-1951(94)00245-5, 1995.

Yalciner, A. C., Synolakis, C., Borrero, J., Altinok, Y., Watts, P., Imamura, F., ... and Tinti, S.: Tsunami generation in Izmit Bay by the 1999 Izmit earthquake, Conferance on the 1999 Kocaeli Earthquake, pp. 217-221, Istanbul Technical University, Istanbul, Turkey, 1999.

Yalciner, A. C., Altinok, Y., Synolakis, C. E., Borrero, J., Imamura, F., Ersoy, S., ... and Yuksel, Y.: Tsunami waves in İzmit 775 Bay, Earthquake Spectra 16(S1), 55-62, 2000.

Yalçıner, A. C., Alpar, B., Altınok, Y., Özbay, İ., and Imamura, F.: Tsunamis in the Sea of Marmara: Historical documents for the past, models for the future, Marine Geology 190(1-2), 445-463, https://doi.org/10.1016/S0025-3227(02)00358-4, 2002.

Yaltırak, C.: Tectonic evolution of the Marmara Sea and its surroundings, Marine Geology 190(1-2), 493-529, 780 https://doi.org/10.1016/S0025-3227(02)00360-2, 2002.

Yalçıner, A., Annunziato, A., Papadopoulos, G., Dogan, G. G., Guler, H. G., Cakir, T. E., and Kanoglu, U.: The 20th July 2017 (22: 31 UTC) Bodrum-Kos Earthquake and Tsunami: Post Tsunami Field Survey Report, 10.13140/RG.2.2.18314.57287, 2017.

Youngs, R. R., and Coppersmith, K. J.: Implications of fault slip rates and earthquake recurrence models to probabilistic 785 seismic hazard estimates, Bulletin of the Seismological society of America, 75(4), 939-964, 1985.

Zolfaghari, M. R.: Development of a synthetically generated earthquake catalogue towards assessment of probabilistic seismic hazard for Tehran, Natural Hazards, 76(1), 497-514, https://doi.org/10.1007/s11069-014-1500-1, 2015.